

Supramolecular Daisy Chains[†]Stuart J. Cantrill,[‡] Gilmer J. Youn, and J. Fraser Stoddart*

Department of Chemistry and Biochemistry, University of California, Los Angeles, California 90095

David J. Williams*

Department of Chemistry, Imperial College, South Kensington, London SW7 2AY, UK

stoddart@chem.ucla.edu

Received April 19, 2001

Two series of self-complementary daisy chain monomers, in which a secondary ammonium ion-containing arm is grafted onto a macrocycle with either a [24]- or [25]crown-8 constitution, have been synthesized. In the solid- and 'gas'-phases, the parent [24]crown-8-based monomer forms dimeric superstructures, as revealed by X-ray crystallography and mass spectrometry, respectively. Elucidation of the complicated solution-phase behavior of this compound was facilitated by the synthesis and study of both deuterated, and fluorinated, analogues. These investigations revealed that the cyclic dimeric superstructure also dominates in solution, except when extremes of either concentration (low), temperature (high), or solvent polarity (highly polar, e.g., dimethyl sulfoxide) are employed. Whereas, upon aggregation, the [24]crown-8-based daisy chain monomers have the capacity to form stereoisomeric superstructures further complicating the study of this series of compounds. The assembly of [25]crown-8-based monomers gives only achiral superstructures. The weaker association exhibited between secondary dialkylammonium ions and crown ethers with a [25]crown-8 constitution, however, resulted in limited oligomerization—only dimeric and trimeric superstructures were formed at experimentally attainable concentrations—of [25]crown-8-based daisy chain monomers.

Introduction

The rise of supramolecular chemistry¹, and its precise exploitation of delicate noncovalent interactions, has spurred investigations² into alternative approaches for polymer synthesis, challenging³ the covalent bond's monopoly of the macromolecular world. Whereas *molecular* polymerization relies upon the formation (Figure 1, top) of *covalent* bonds between monomeric building blocks, the propagation step in a *supramolecular* polymerization proceeds via the formation (Figure 1, bottom) of *noncovalent* bonds. Consequently, it is the inherent reversibility associated with the self-assembly⁴ of such a dynamic aggregate that is anticipated⁵ to bestow, upon the resulting polymer, properties that are distinct from those observed for traditional covalently linked macromolecules. Foremost, polymerization performed under such a thermodynamically controlled regime allows^{2c,5} for a high degree of architectural control; incorrect or

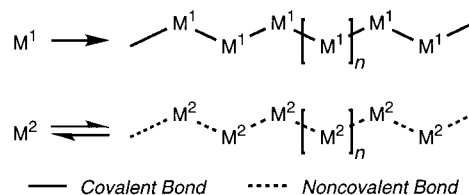


Figure 1. Top: A schematic representation of the covalent polymerization of monomer M^1 . Bottom: A schematic representation of the noncovalent polymerization of a different monomer, M^2 .

unspecific chain extensions are simply reversed in the constantly evolving system as it strives to find a local energy minimum. Furthermore, once assembled, the dynamic nature of such an assembly does not cease to be important. In fact, this very attribute remains of paramount importance, and renders such a species extremely sensitive (i.e., responsive) to external environmental factors⁵ such as mechanical stress or temperature. Once sheared, a material linked through noncovalent

* To whom correspondence should be addressed. Tel: (310) 206 7078. Fax: (310) 206 1843.

[†] Molecular Meccano, Part 64. For Part 63, see: Ashton, P. R.; Baldoni, V.; Balzani, V.; Credi, A.; Hoffmann, H. D. A.; Martinez-Diaz, M.-V.; Raymo, F. M.; Stoddart, J. F.; Venturi, M. *Chem. Eur. J.* **2001**, *7*, 3482–3493.

[‡] Current address: Division of Chemistry and Chemical Engineering, California Institute of Technology, Pasadena, CA 91125.

(1) (a) Lehn, J.-M. *Supramolecular Chemistry*; VCH: Weinheim, 1995. (b) *Comprehensive Supramolecular Chemistry*; Atwood, J. L.; Davies, J. E. D.; MacNicol, D. D.; Vögtle, F., Eds.; Pergamon: Oxford, 1996; 11 vols.

(2) (a) Archer, R. D. *Coord. Chem. Rev.* **1993**, *128*, 49–68. (b) Rehahn, M. *Acta Polymer.* **1998**, *49*, 201–224. (c) Moore, J. S. *Curr. Opin. Colloid Interface Sci.* **1999**, *4*, 108–116. (d) *Supramolecular Polymers*; Ciferri, A., Ed.; Marcel Dekker: New York, 2000.

(3) Zimmerman, N.; Moore, J. S.; Zimmerman, S. C. *Chem. Ind.* **1998**, 604–610.

(4) (a) Whitesides, G. M.; Mathias, J. P.; Seto, C. T. *Science* **1991**, *154*, 1312–1319. (b) Lawrence, D. S.; Jiang, T.; Levett, M. *Chem. Rev.* **1995**, *95*, 2229–2260. (c) Philp, D.; Stoddart, J. F. *Angew. Chem., Int. Ed. Engl.* **1996**, *35*, 1154–1196. (d) Stang, P. J.; Olenyuk, B. *Acc. Chem. Res.* **1997**, *30*, 502–518. (e) Conn, M. M.; Rebek, J., Jr. *Chem. Rev.* **1997**, *97*, 1647–1668. (f) Linton, B.; Hamilton, A. D. *Chem. Rev.* **1997**, *97*, 1669–1680. (g) Fujita, M. *Chem. Soc. Rev.* **1998**, *27*, 417–425. (h) Emrick, T.; Fréchet, J. M. J. *Curr. Opin. Colloid Interface Sci.* **1999**, *4*, 15–23. (i) Sijbesma, R. P.; Meijer, E. W. *Curr. Opin. Colloid Interface Sci.* **1999**, *4*, 24–32. (j) Lindoy, L. F.; Atkinson, I. M. *Self-Assembly in Supramolecular Systems*; Stoddart, J. F., Ed.; RSC: Cambridge, 2000.

(5) Sijbesma, R. P.; Beijer, F. H.; Brunsveld, L.; Folmer, B. J. B.; Ky Hirschberg, J. H. K.; Lange, R. F. M.; Lowe, J. K. L.; Meijer, E. W. *Science* **1997**, *278*, 1601–1604.

interactions retains, under the appropriate conditions, the capacity to 'heal' itself, reforming those bonds that were broken under the application of mechanical stress. Conversely, no correspondingly simple repair mechanism exists for covalent polymers. Second, changes in temperature should affect⁶ directly (and reversibly) the degree of polymerization (DP) exhibited by a supramolecular polymer, and in turn, may be used to attenuate bulk properties such as viscosity and/or rheology. In contrast, although potentially significant,⁷ temperature effects upon covalent polymers are generally less dramatic and are rarely⁸ utilized in order to alter, reversibly, the degree of polymerization.

Although both (i) metal–ligand,^{6,9} and (ii) π – π stacking¹⁰ interactions have been utilized as the 'glue' with which monomers have been strung together to form supramolecular polymers, hydrogen bonding interactions have been exploited^{5,11–15} far more widely. This prefer-

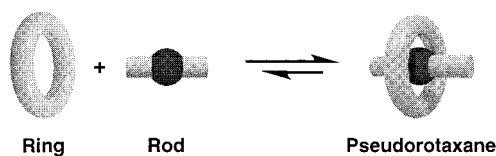


Figure 2. A schematic representation depicting the formation of a threaded 1:1 complex (a pseudorotaxane) between two complementary species wherein the cavity of a suitably sized ring is skewered by a linear rod.

ence arises as a consequence of the easily tunable, and therefore favorable, thermodynamic and kinetic parameters associated with hydrogen bonding interactions. Whereas the reversibility of some metal–ligand interactions is limited, and the strength of π – π stacking interactions is not sufficient enough to produce polymers with high DPs, hydrogen bonding interactions can be fine-tuned to deliver the desired properties. Although single,¹¹ double,¹² and triple¹³ hydrogen bond manifolds have been employed in the construction of supramolecular polymers, the most successful has been that involving a quadruple¹⁴ couple. Meijer and co-workers have exploited the strong dimerization¹⁶ of 2-ureido-4-pyrimidone derivatives, with K_a values in excess of 10^6 M^{-1} in CHCl_3 , for the reversible formation¹⁴ of hydrogen-bonded supramolecular polymers and networks.

Rather than the simple face-to-face association (vide supra) of monomers, however, more complex topological interactions may be contrived. The concept (Figure 2) of threading a rod-shaped molecule through the macrocyclic cavity of another ring-shaped one—to create¹⁷ an interwoven host–guest complex (often referred to as a pseudorotaxane¹⁸)—can be applied to the propagation step of a supramolecular polymerization. Covalently coupling the two mutually recognizing components to one another¹⁹ affords (Figure 3) a self-complementary mono-

(6) The degree of polymerization (DP) depends critically upon the association constant (K_a) for two monomer units (see: Michelsen, U.; Hunter, C. A. *Angew. Chem., Int. Ed.* **2000**, *39*, 764–767) and can be approximated by using the following expression: $\text{DP} \approx \sqrt{(K_a[\text{monomer}])}$. Consequently, since $K_a = (\Delta S - \Delta H)/RT$, changing the temperature can alter dramatically the value of K_a , and hence also that of DP.

(7) For recent examples of thermoresponsive polymers, see: (a) Everlof, G. J.; Jaycox, G. D. *Polymer* **2000**, *41*, 6527–6536. (b) Bignotti, F.; Penco, M.; Sartore, L.; Peroni, I.; Mendichi, R.; Casolaro, M.; D'Amore, A. *Polymer* **2000**, *41*, 8247–8256. (c) Pan, H.-Z.; Yan, Y.; Tang, L.; Wu, Z.-Q.; Li, F.-M. *Macromol. Rapid Commun.* **2000**, *21*, 567–573. (d) Kurisawa, M.; Yokoyama, M.; Okano, T. *J. Controlled Release* **2000**, *69*, 127–137. (e) Kim, S. Y.; Cho, S. M.; Lee, Y. M.; Kim, S. J. *J. Appl. Polym. Sci.* **2000**, *78*, 1381–1391.

(8) The exception to this statement relates to equilibrium polymerizations, in which dynamic covalent chemistry is employed for the reversible formation of covalently bonded polymers. For a general background on this topic, see: (a) Sawada, H. J. *Macromol. Sci. Rev. Macromol. Chem.* **1972**, *C8*, 235–288. For specific examples describing how temperature effects can be used to control the DP in a given polymer system, see: (b) Chikaoka, S.; Takata, T.; Endo, T. *Macromolecules* **1991**, *24*, 6557–6562. (c) Marsella, M. J.; Maynard, H. D.; Grubbs, R. H. *Angew. Chem., Int. Ed. Engl.* **1997**, *36*, 1101–1103. (d) Lowe, T. L.; Tenhu, H. *Macromolecules* **1998**, *31*, 1590–1594.

(9) (a) Constable, E. C. *Chem. Commun.* **1997**, 1073–1080. (b) Kelch, S.; Rehahn, M. *Macromolecules* **1997**, *30*, 6185–6193. (c) Kelch, S.; Rehahn, M. *Macromolecules* **1999**, *32*, 5818–5828. (d) Gardner, M.; Guerin, A. J.; Hunter, C. A.; Michelsen, U.; Rotger, C. *New J. Chem.* **1999**, 309–316. (e) Wojaczynski, J.; Latos-Grazynski, L. *Coord. Chem. Rev.* **2000**, *204*, 113–171. (f) Ogawa, K.; Kobuke, Y. *Angew. Chem., Int. Ed.* **2000**, *39*, 4070–4073. (g) Ellis, W. W.; Schmitz, M.; Arif, A. A.; Stang, P. J. *Inorg. Chem.* **2000**, *39*, 2547–2557. In contrast with these metallo-supramolecular polymers, which exhibit macromolecular properties in solution, much research has been done on the crystal engineering of solid-state coordination networks that are also referred to as 'polymers'. See: (h) Hirsch, K. A.; Wilson, S. R.; Moore, J. S. *Inorg. Chem.* **1997**, *36*, 2960–2968. (i) Blake, A. J.; Champness, N. R.; Hubberstey, P.; Li, W. S.; Withersby, M. A.; Schroder, M. *Coord. Chem. Rev.* **1999**, *183*, 117–138. (j) Shimizu, G. K. H.; Enright, G. D.; Rego, G. S.; Ripmeester, J. A. *Can. J. Chem.* **1999**, *77*, 313–318. (k) Carlucci, L.; Ciani, G.; Proserpio, D. M. *Chem. Commun.* **1999**, 449–450. (l) Groeneman, R. H.; MacGillivray, L. R.; Atwood, J. L. *Inorg. Chem.* **1999**, *38*, 208–209. (m) Gudbjartson, H.; Biradha, K.; Poirier, K. M.; Zaworotko, M. J. *J. Am. Chem. Soc.* **1999**, *121*, 2599–2600. (n) Kleina, C.; Graf, E.; Hosseini, M. W.; De Cian, A.; Fischer, J. *Chem. Commun.* **2000**, 239–240. (o) Hong, M.; Zhao, Y.; Su, W.; Cao, R.; Fujita, M.; Zhou, Z.; Chan, A. S. C. *Angew. Chem., Int. Ed.* **2000**, *39*, 2468–2470. (p) Robson, R. *J. Chem. Soc., Dalton Trans.* **2000**, 3735–3744. (q) Biradha, K.; Fujita, M. *J. Chem. Soc., Dalton Trans.* **2000**, 3805–3810. (r) Sharma, A. C.; Borovik, A. S. *J. Am. Chem. Soc.* **2000**, *122*, 8946–8955.

(10) (a) Alcock, N. W.; Barker, P. R.; Haider, J. M.; Hannon, M. J.; Painting, C. L.; Pikramenou, Z.; Plummer, E. A.; Rissanen, K.; Saarenketo, P. *J. Chem. Soc., Dalton Trans.* **2000**, 1447–1461. (b) Hirschberg, J. H. K. K.; Brunsveld, L.; Ramzi, A.; Vekemans, J. A. J. M.; Sijbesma, R. P.; Meijer, E. W. *Nature* **2000**, *407*, 167–170.

(11) (a) Bladon, P.; Griffin, A. C. *Macromolecules* **1993**, *26*, 6604–6610. (b) Alexander, C.; Jariwala, C. P.; Lee, C. M.; Griffin, A. C. *Macromol. Symp.* **1994**, *77*, 283–294. (c) Lee, C. M.; Jariwala, C. P.; Griffin, A. C. *Polymer* **1994**, *35*, 4550–4554. (d) St Pourcain, C. B.; Griffin, A. C. *Macromolecules* **1995**, *28*, 4116–4121. (e) Lee, C. M.; Griffin, A. C. *Macromol. Symp.* **1997**, *117*, 281–290.

(12) (a) Ducharme, Y.; Wuest, J. D. *J. Org. Chem.* **1988**, *53*, 5787–5789. (b) Lillya, C. P.; Baker, R. J.; Hutte, S.; Winter, H. H.; Lin, Y. G.; Shi, J. F.; Dickinson, L. C.; Chen, J. C. W. *Macromolecules* **1992**, *25*, 2076–2080. (c) Abed, S.; Boileau, S.; Bouteiller, L. *Macromolecules* **2000**, *33*, 8479–8487.

(13) (a) Kotera, M.; Lehn, J.-M.; Vigneron, J.-P. *J. Chem. Soc., Chem. Commun.* **1994**, 197–199. (b) Russell, K. C.; Lehn, J.-M.; Kyritsakas, N.; DeCian, A.; Fischer, J. *New J. Chem.* **1998**, 123–128. (c) Choi, I. S.; Li, X.; Simanek, E. E.; Akaba, R.; Whitesides, G. M. *Chem. Mater.* **1999**, *11*, 684–690. (d) Klok, H.-A.; Jolliffe, K. A.; Schauer, C. L.; Prins, L. J.; Spatz, J. P.; Möller, M.; Timmerman, P.; Reinholdt, D. N. *J. Am. Chem. Soc.* **1999**, *121*, 7154–7155.

(14) (a) Folmer, B. J. B.; Cavini, E.; Sijbesma, R. P.; Meijer, E. W. *Chem. Commun.* **1998**, 1847–1848. (b) Hirschberg, J. H. K. K.; Beijer, F. H.; van Aert, H. A.; Magusim, P. C. M. M.; Sijbesma, R. P.; Meijer, E. W. *Macromolecules* **1999**, *32*, 2696–2705. (c) Lange, R. F. M.; Van Gurp, M.; Meijer, E. W. *J. Polym. Sci., Part A: Polym. Chem.* **1999**, *37*, 3657–3670. (d) Folmer, B. J. B.; Sijbesma, R. P.; Versteegen, R. M.; van der Rijt, J. A. J.; Meijer, E. W. *Adv. Mater.* **2000**, *12*, 874–878. (e) Boileau, S.; Bouteiller, L.; Lauprêtre, F.; Lortie, F. *New J. Chem.* **2000**, 845–848. (f) Folmer, B. J. B.; Sijbesma, R. P.; Meijer, E. W. *J. Am. Chem. Soc.* **2001**, *123*, 2093–2094.

(15) (a) Castellano, R. K.; Rudkevich, D. M.; Rebek, J., Jr. *Proc. Natl. Acad. Sci. U.S.A.* **1997**, *94*, 7132–7137. (b) Castellano, R. K.; Rebek, J., Jr. *J. Am. Chem. Soc.* **1998**, *120*, 3657–3663. (c) Castellano, R. K.; Rebek, J., Jr. *Polym. Mater. Sci. Eng.* **1999**, *80*, 16–17. (d) Castellano, R. K.; Nuckolls, C.; Eichhorn, S. H.; Wood, M. R.; Lovinger, A. J.; Rebek, J., Jr. *Angew. Chem., Int. Ed.* **1999**, *38*, 2603–2606.

(16) (a) Beijer, F. H.; Kooijman, H.; Spek, A. L.; Sijbesma, R. P.; Meijer, E. W. *Angew. Chem., Int. Ed.* **1998**, *37*, 75–78. (b) Beijer, F. H.; Sijbesma, R. P.; Kooijman, H.; Spek, A. L.; Meijer, E. W. *J. Am. Chem. Soc.* **1998**, *120*, 6761–6769. (c) El-ghayoury, A.; Peeters, E.; Schenning, A. P. H. J.; Meijer, E. W. *Chem. Commun.* **2000**, 1969–1970. For other recent examples of self-complementary quadruple hydrogen-bonded dimers yet to be utilized in the construction of larger aggregates, see: (d) Corbin, P. S.; Zimmerman, S. C. *J. Am. Chem. Soc.* **1998**, *120*, 9710–9711. (e) Davis, A. P.; Draper, S. M.; Dunne, G.; Ashton, P. R. *Chem. Commun.* **1999**, 2265–2266.

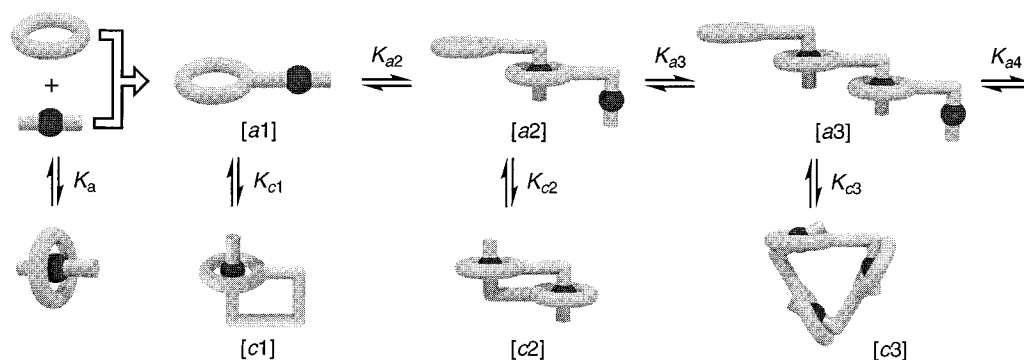


Figure 3. Conceptually, when two mutually recognizing species are merged together, a single self-complementary entity is formed. This daisy-chain monomer can then self-assemble to form both cyclic (*c*) and acyclic (*a*) interwoven superstructures. Note: the numerical descriptor refers to the number of monomer units that make up any particular superstructure, i.e., a cyclic dimer is a [*c*2]daisy chain.

mer,²⁰ which has the capacity to self-assemble into either linear²¹ or cyclic²² daisy chain²³ arrays.²⁴ The research reported in this paper focuses upon the study of self-complementary molecules containing both crown ether and dibenzylammonium ion recognition sites. The design, synthesis, characterization, and ultimately aggregation behavior of these daisy chain monomers, which are based upon a well-understood²⁵ supramolecular interaction, are described.

Results and Discussion

[24]Crown-8-Based Systems. Conceptually, the initial target molecule (**1-H-PF₆**) arose as a consequence of

(17) For recent examples, see: (a) Jeon, Y. M.; Whang, D.; Kim, J.; Kim, K. *Chem. Lett.* **1996**, 503–504. (b) Mirzozian, A.; Kaifer, A. E. *Chem. Eur. J.* **1997**, *3*, 1052–1058. (c) Sleiman, H.; Baxter, P. N. W.; Lehn, J.-M.; Airola, K.; Rissanen, K. *Inorg. Chem.* **1997**, *36*, 4734–4742. (d) Loeb, S. J.; Wisner, J. A. *Angew. Chem., Int. Ed.* **1998**, *37*, 2838–2840. (e) Smith, A. C.; Macartney, D. H. *J. Org. Chem.* **1998**, *63*, 9243–9251. (f) Asakawa, M.; Ashton, P. R.; Balzani, V.; Boyd, S. E.; Credi, A.; Mattersteig, G.; Menzer, S.; Montalti, M.; Raymo, F. M.; Ruffilli, C.; Stoddart, J. F.; Venturi, M.; Williams, D. J. *Org. Chem.* **1999**, *985*, 5–994. (g) Cantrill, S. J.; Fyfe, M. C. T.; Heiss, A. M.; Stoddart, J. F.; White, A. J. P.; Williams, D. J. *Org. Lett.* **2000**, *2*, 61–64. (h) Chang, T.; Heiss, A. M.; Cantrill, S. J.; Fyfe, M. C. T.; Pease, A. R.; Rowan, S. J.; Stoddart, J. F.; Williams, D. J. *Org. Lett.* **2000**, *2*, 2943–2946. (i) Chang, T.; Heiss, A. M.; Cantrill, S. J.; Fyfe, M. C. T.; Pease, A. R.; Rowan, S. J.; Stoddart, J. F.; White, A. J. P.; Williams, D. J. *Org. Lett.* **2000**, *2*, 2947–2950. (j) Ryan, D.; Rao, S. N.; Rensmo, H.; Fitzmaurice, D.; Preece, J. A.; Wenger, S.; Stoddart, J. F.; Zacheroni, N. J. *Am. Chem. Soc.* **2000**, *122*, 6252–6257. (k) Chichak, K.; Walsh, M. C.; Branda, N. R. *Chem. Commun.* **2000**, 847–848.

(18) These complexes, in which an acyclic component is threaded through a cyclic one, are simply rotaxanes which are lacking the bulky end-groups, and are, therefore, termed *pseudorotaxanes*. In fact, pseudorotaxanes occupy a pivotal position in the chemistry of mechanically interlocked compounds, as they can serve as intermediates in the syntheses of both catenanes and rotaxanes. For recent examples, see: (a) Hansen, J. G.; Feeder, N.; Hamilton, D. G.; Gunter, M. J.; Becher, J.; Sanders, J. K. M. *Org. Lett.* **2000**, *2*, 449–452. (b) Raehm, L.; Hamann, C.; Kern, J.-M.; Sauvage, J.-P. *Org. Lett.* **2000**, *2*, 1991–1994. (c) Safarowsky, O.; Vogel, E.; Vögtle, F. *Eur. J. Org. Chem.* **2000**, 499–505. (d) Cabezon, B.; Cao, J.; Raymo, F. M.; Stoddart, J. F.; White, A. J. P.; Williams, D. J. *Chem. Eur. J.* **2000**, *6*, 2262–2273. (e) Reuter, C.; Vögtle, F. *Org. Lett.* **2000**, *2*, 593–595. (f) Skinner, P. J.; Blair, S.; Katakya, R.; Parker, D. *New J. Chem.* **2000**, *24*, 265–268. (g) Kawaguchi, Y.; Harada, A. *Org. Lett.* **2000**, *2*, 1353–1356. (h) Loeb, S. J.; Wisner, J. A. *Chem. Commun.* **2000**, 845–846. (i) Buston, J. E. H.; Young, J. R.; Anderson, H. L. *Chem. Commun.* **2000**, 905–906. (j) Cantrill, S. J.; Fulton, D. A.; Heiss, A. M.; Pease, A. R.; Stoddart, J. F.; White, A. J. P.; Williams, D. J. *Chem. Eur. J.* **2000**, *6*, 2274–2287. (k) Tachibana, Y.; Kihara, N.; Ohga, Y.; Takata, T. *Chem. Lett.* **2000**, 806–807.

(19) An alternative approach requires the self-assembly of two homoditopic monomers, i.e., AA and BB building blocks, rather than a self-complementary AB one. See: (a) Yamaguchi, N.; Gibson, H. W. *Angew. Chem., Int. Ed.* **1999**, *38*, 143–147. (b) Yamaguchi, N.; Gibson, H. W. *Chem. Commun.* **1999**, 789–790. Interwoven supramolecular polymers constructed in this fashion would serve as precursors for a novel interlocked macromolecular architecture, recently termed a 'Figure 8 polyrotaxane' by Busch et al. See: Hubin, T. J.; Kolchinski, A. G.; Vance, A. L.; Busch, D. H. *Adv. Supramol. Chem.* **1999**, *10*, 237–357.

(20) (a) Ashton, P. R.; Baxter, I.; Cantrill, S. J.; Fyfe, M. C. T.; Glink, P. T.; Stoddart, J. F.; White, A. J. P.; Williams, D. J. *Angew. Chem., Int. Ed.* **1998**, *37*, 1294–1297. (b) Ashton, P. R.; Parsons, I. W.; Raymo, F. M.; Stoddart, J. F.; White, A. J. P.; Williams, D. J.; Wolf, R. *Angew. Chem., Int. Ed.* **1998**, *37*, 1913–1916. (c) Yamaguchi, N.; Nagvekar, D. S.; Gibson, H. W. *Angew. Chem., Int. Ed.* **1998**, *37*, 2361–2364. (d) Mirzozian, A.; Kaifer, A. E. *Chem. Commun.* **1999**, 1603–1604. (e) Bülger, J.; Sommerdijk, N. A. J. M.; Visser, A. J. W. G.; van Hoek, A.; Nolte, R. J. M.; Engbersen, J. F. J.; Reinhoudt, D. N. *J. Am. Chem. Soc.* **1999**, *121*, 28–33. (f) Nielsen, M. B.; Hansen, J. G.; Becher, J. *Eur. J. Org. Chem.* **1999**, 2807, 7–2815. (g) Jiménez, M. C.; Dietrich-Buchecker, C.; Sauvage, J.-P.; De Cian, A. *Angew. Chem., Int. Ed.* **2000**, *39*, 1295–1298.

(21) Appropriately monosubstituted cyclo-oligosaccharides have been shown to crystallize to give arrays of this type in the solid state, see: (a) Hirotsu, K.; Higuchi, T.; Fujita, K.; Ueda, T.; Shinoda, A.; Imoto, T.; Tabushi, I. *J. Org. Chem.* **1982**, *47*, 1143–1144. (b) Mentzafos, D.; Terzis, A.; Coleman, A. W.; de Rango, C. *Carbohydr. Res.* **1996**, *282*, 125–135. (c) Liu, Y.; You, C.-C.; Zhang, M.; Weng, L.-H.; Wada, T.; Inoue, Y. *Org. Lett.* **2000**, *2*, 2761–2763.

(22) Cyclic arrays are formed whenever chain termination of a propagating acyclic species occurs via intramolecular 'back-biting'. For examples, see: ref 20a,b,d,g. In some less geometrically demanding cases, the monomeric species is also capable of biting its own tail, to form an intramolecular self-complexed species. See: ref 20e,f, and Ashton, P. R.; Ballardini, R.; Balzani, V.; Boyd, S. E.; Credi, A.; Gandolfi, M. T.; Gómez-López, M.; Iqbal, S.; Philp, D.; Preece, J. A.; Prodi, L.; Ricketts, H. G.; Stoddart, J. F.; Tolley, M. S.; Venturi, M.; White, A. J. P.; Williams, D. J. *Chem. Eur. J.* **1997**, *3*, 152–170.

(23) The term 'daisy chain' is used to describe an interwoven chain, usually made of flowers (hence 'daisy'), in which each unit acts as a 'donor' and an 'acceptor' for a threading interaction. The standard definition (*Webster's Third New International Dictionary*; Babcock-Gove, P., Ed.; Merriam-Webster: Springfield MA, 1993) of a 'daisy chain' is: "a string of daisies with stems linked to form a chain,..... such a chain carried by chosen students at a class day or other celebration in some women's colleges". With regard to chemical systems, it should be noted that Busch and co-workers coined their own term for such a supramolecular polymeric architecture, calling it a 'Figure 9 pseudo-polyrotaxane'. See: Hubin, T. J.; Busch, D. H. *Coord. Chem. Rev.* **2000**, *200–202*, 5–52.

(24) Small cyclic daisy chain structures have been trapped kinetically upon postassembly covalent modification of the corresponding complexes. For examples of dimers, see: (a) Jiménez, M. C.; Dietrich-Buchecker, C.; Sauvage, J.-P. *Angew. Chem., Int. Ed.* **2000**, *39*, 3284–3287. (b) Fujimoto, T.; Sakata, Y.; Kaneda, T. *Chem. Commun.* **2000**, 2143–2144. (c) Onagi, H.; Easton, C. J.; Lincoln, S. F. *Org. Lett.* **2001**, *3*, 1041–1044. For a captured trimer, see: (d) Hoshino, T.; Miyauchi, M.; Kawaguchi, Y.; Yamaguchi, H.; Harada, A. *J. Am. Chem. Soc.* **2000**, *122*, 9876–9877. An alternative approach for the construction of these novel mechanically interlocked assemblies, which relies upon covalent, rather than noncovalent, oligo/polymerization, was communicated before any of the above reports. See: (e) Rowan, S. J.; Cantrill, S. J.; Stoddart, J. F.; White, A. J. P.; Williams, D. J. *Org. Lett.* **2000**, *2*, 759–762.

(25) Ashton, P. R.; Chrystal, E. J. T.; Glink, P. T.; Menzer, S.; Schiavo, C.; Spencer, N.; Stoddart, J. F.; Tasker, P. A.; White, A. J. P.; Williams, D. J. *Chem. Eur. J.* **1996**, *2*, 709–728.

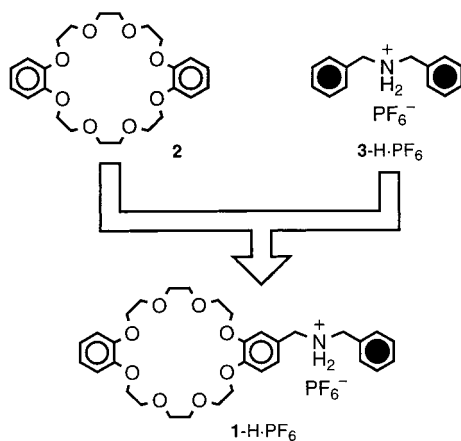


Figure 4. Combining the features of both DB24C8 (**2**) and dibenzylammonium hexafluorophosphate (**3-H·PF₆**) into one and the same molecule results in the design of a self-complementary daisy chain monomer **1-H·PF₆**.

splicing (Figure 4) both the dibenzo[24]crown-8 (**2**) and dibenzylammonium hexafluorophosphate (**3-H·PF₆**) structural motifs into one and the same molecule. Upon inspection of space-filling molecular models, it was apparent that such a structure satisfied one of the most important design criteria, i.e., that intramolecular self-complexation is geometrically unfavorable, if not impossible.

The Parent Monomer. The synthesis of this self-complementary daisy chain monomer is outlined in Scheme 1. Alkylation of 3,4-dihydroxybenzaldehyde (**4**) with the chloride **5** proceeded under basic conditions in DMF to afford the diol **6** in very good yield. Tosylation of **6**, under standard conditions, gave the ditosylate **7**, which was subsequently reacted with catechol (**8**) to give the formyl-substituted DB24C8 derivative **9** in reasonable yield. Condensation of **9** with benzylamine (**10**), followed by borohydride reduction, protonation (HCl), and counterion exchange from Cl⁻ to PF₆⁻, afforded the target compound **1-H·PF₆** in a 73% yield.

Mass Spectrometry. The liquid secondary ion (LSI) mass spectrum of the salt **1-H·PF₆** revealed (Figure 5) intense peaks, encountered at $m/z = 1281$ and 1135 , corresponding to the creation of dimeric supermolecules in the 'gas phase'. These peaks can be identified as the supramolecular ions $[(1-H)_2(PF_6)]^+$ and $[(1-H)(1)]^+$, respectively, and indicate the aggregation of two monomer units. The peak at $m/z = 1135$ was observed to be the spectrum's base peak—it was approximately twice as

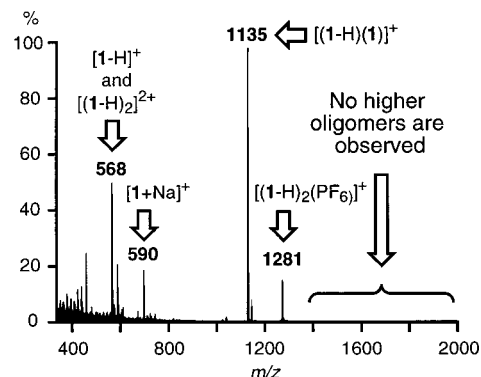
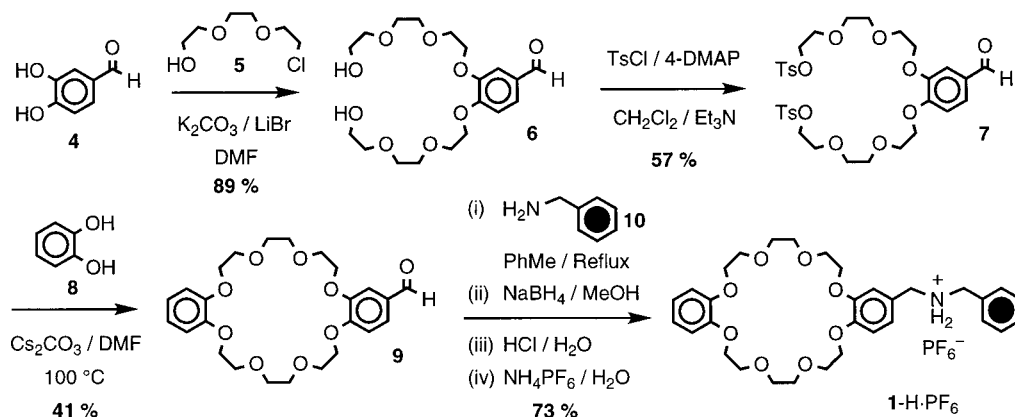


Figure 5. The LSI-mass spectrum of **1-H·PF₆**.

intense as the peak located at $m/z = 568$, which could correspond to the species $[1-H]^+$. However, closer inspection of the expanded spectrum revealed that the isotope peaks, in the area surrounding the $[1-H]^+$ peak, are separated by 0.5 mass units, indicating the presence of a doubly charged species with a mass corresponding to a dimeric entity, thus providing evidence for the existence of the doubly charged dimer $[(1-H)_2]^{2+}$. It is also notable that no higher order oligomeric species were detected, inferring that they are either (i) not formed, (ii) do not survive the conditions of the analysis, or (iii) are not amenable to mass spectrometric analysis, i.e., do not ionize as well as their smaller siblings.

X-ray Crystallography. The trifluoroacetate²⁶ salt **1-H·O₂CCF₃** crystallized^{20a} on standing from a mixture of (EtOAc/C₆H₁₄/CD₃CN, ca. 10:10:1) affording crystals suitable for single-crystal X-ray diffraction analysis. The X-ray structural analysis of **1-H·O₂CCF₃** revealed (Figure 6) the formation of a *C*₂ symmetric head-to-tail dimeric structure in which the benzylammonium cationic portions of each component thread simultaneously through the DB24C8 portions of their adjacent counterparts. The pairs of molecules are stabilized by a combination of π - π stacking of the substituted catechol rings (interplanar and centroid-centroid separations of 3.36 and 3.55 Å, respectively) and $[N^+ \cdots H \cdots O]$ hydrogen bonds between one of the hydrogen atoms on each NH₂⁺ center and a polyether oxygen atom within one of the linkages of each DB24C8 component ($[N^+ \cdots O]$, $[H \cdots O]$ distances are 2.91 and 2.02 Å, respectively, with an $[N^+ - H \cdots O]$ angle of 170°). Interestingly, in this instance, the interaction between the two achiral **1-H**⁺ cations is dissymmetrizing, rendering a chiral association and resulting in the formation (Figure 7a,c) of a pair of enantiomeric *C*₂-

Scheme 1. The Synthesis of the Parent [24]Crown-8 Daisy-Chain Monomer 1-H·PF₆



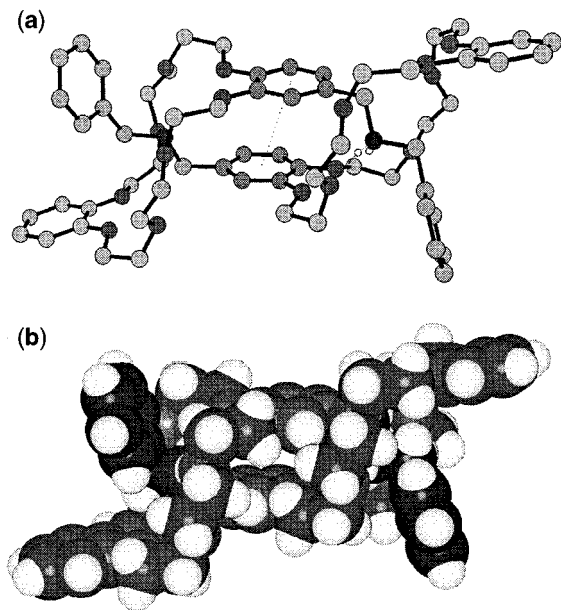


Figure 6. (a) Ball-and-stick and (b) space-filling representations of the C_2 symmetric head-to-tail dimer formed by 1-H^+ .

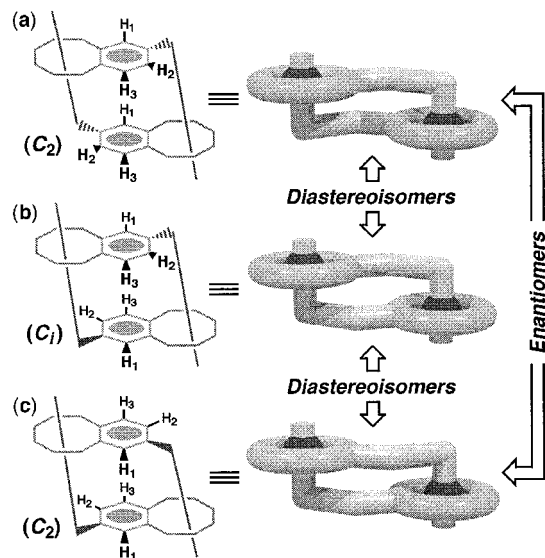


Figure 7. The three cyclic stereoisomeric superstructures that can be formed upon dimerization of $1\text{-H}\cdot\text{PF}_6$.

symmetric supramolecular stereoisomers. This kind of interaction occurs because the enantiotopic faces of the interacting 1-H^+ cations possess the same prochirality. However, an alternative situation can also be envisaged: a diastereoisomeric 'meso' supramolecular stereoisomer, endowed with C_i symmetry, would have been created (Figure 7b) if the interacting faces of individual 1-H^+ cations had maintained different prochiralities upon crystallization. In other words, the noncovalent dimerization of the 1-H^+ cation proceeds diastereoselectively, at least in the solid state, to furnish a racemic mixture of the C_2 -symmetric supramolecular stereoisomers.

NMR Spectroscopy. The ^1H NMR spectrum (300 MHz, 298 K) of the hexafluorophosphate salt $1\text{-H}\cdot\text{PF}_6$,

(26) Despite repeated efforts, the PF_6^- salt of 1^+ would not crystallize to give material of suitable quality for single-crystal X-ray analysis. However, on changing to the CF_3CO_2^- anion, good crystals were obtained easily.

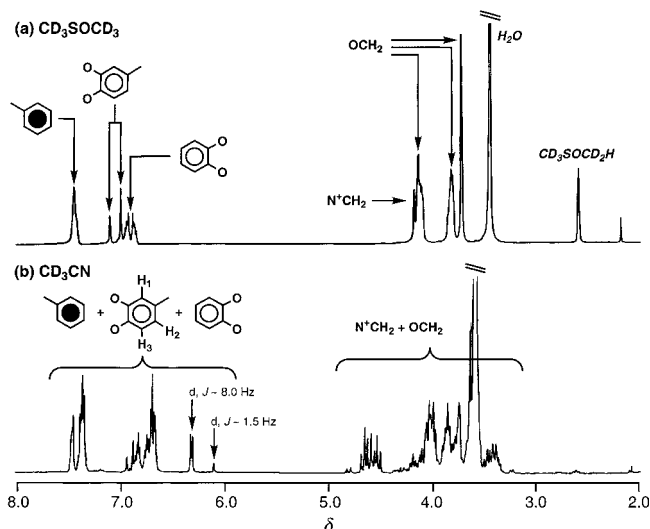


Figure 8. The ^1H NMR spectra of $1\text{-H}\cdot\text{PF}_6$ dissolved in (a) CD_3SOCD_3 (300 MHz, 298 K), and (b) CD_3CN (400 MHz, 273 K).

recorded in CD_3SOCD_3 , is shown in Figure 8a. The spectrum is relatively simple, and each of the peaks can be assigned (as annotated in the figure) as arising from a particular set of protons. In contrast, however, when the ^1H NMR spectrum (400 MHz, 273 K) of $1\text{-H}\cdot\text{PF}_6$ was recorded in CD_3CN , a more complicated spectrum (Figure 8b) was observed. The simpler ' CD_3SOCD_3 ' spectrum can be rationalized by ascribing it to the 'monomeric' daisy chain species, i.e., no complexation is occurring. As expected,²⁵ in the more polar CD_3SOCD_3 , solvation of the ammonium center occurs preferentially by the solvent molecules rather than by the macrocyclic polyether component, thus precluding intermolecular association of the daisy chain monomers. Conversely, in the less polar CD_3CN solution, the preference for complexation of the ammonium center by the solvent is less overwhelming,²⁵ and hence ammonium ion complexation ensues. Consequently the formation of numerous oligomeric species, all in slow exchange²⁷ with one another, could result in the complicated spectrum observed for $1\text{-H}\cdot\text{PF}_6$ in CD_3CN solution.

The only well-resolved peaks in this spectrum are two doublets, with coupling constants of ~ 1.5 and 8.0 Hz, respectively, that have been shifted upfield from the remainder of the signals associated with the aromatic protons. Upon the basis of chemical shift arguments,²⁸ these signals can be assigned to protons attached to the central aromatic ring of $1\text{-H}\cdot\text{PF}_6$; a *meta*-coupled doublet

(27) DB24C8-sized macrocycles and phenyl-terminated secondary ammonium ions form threaded complexes at a rate slower than the ^1H NMR time scale. Consequently, all different species present in solution give rise to their own distinct set of NMR resonances. See: ref 25.

(28) With regard to aromatic proton spin systems, coupling constants of 1.5 and 8.0 Hz suggest *meta* (4J) and *ortho* (3J) coupling, respectively. Therefore, such coupling patterns, as well as δ values, are unlikely to arise from the protons of the terminal benzyl ring; the protons of such an electron neutral (neither especially electron poor nor rich) aromatic ring would be expected to produce signals with δ values of $\sim 7.1\text{--}7.6$ ppm, as well as give rise to a more complicated splitting pattern. Similar logic leads to the same conclusion for the protons of the 'catechol' ring (i.e., the $o\text{-C}_6\text{H}_4\text{O}_2$ aromatic residue) of $1\text{-H}\cdot\text{PF}_6$. Although in an electron rich ring, the resonances of protons attached to 1,2-dioxy-substituted benzene rings generally give rise to second-order multiplets (or occasionally broad singlets) centered around $\delta \sim 6.8\text{--}7.0$ ppm. Therefore, the most plausible explanation is one based upon the protons attached to the central aromatic ring of $1\text{-H}\cdot\text{PF}_6$.

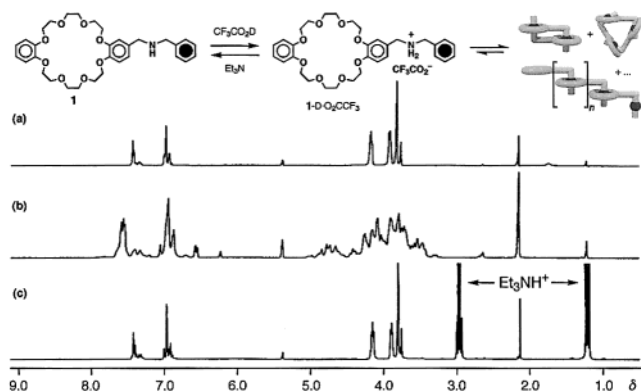


Figure 9. ^1H NMR spectra of (a) the amine **1**, followed by sequential addition of (b) $\text{CF}_3\text{CO}_2\text{D}$ (10 mol equiv), and (c) Et_3N (20 mol equiv).

is expected for H_1 , and an *ortho*-coupled doublet is anticipated for H_3 . The relative upfield shift of these distinctive doublets probably results from the offset face-to-face stacking of two of these central aromatic units, as would be anticipated, based upon observations of the solid-state superstructure (vide supra), for a cyclic head-to-tail dimer. However, the ratio of the intensities of these two doublets is $\sim 5:1$, indicating that they must originate from two *different* cyclic dimeric superstructures. As noted previously, however, three possible stereoisomeric head-to-tail dimers (recall Figure 7) can be formed—an enantiomeric pair and a third diastereoisomeric '*meso*' form. Despite the presence of only the racemate in the solid-state superstructure, this inherently kinetic crystallization process does not rule out the possibility that the '*meso*' diastereoisomer is also present in solution. Hence, one dimeric diastereoisomer may²⁹ position H_3 within a shielding zone, and the other, H_1 .

Acid/Base Effects. The spectrum of the amine **1** is shown in Figure 9a. Upon addition of an excess of $\text{CF}_3\text{CO}_2\text{D}$ (10 mol equiv) to the NMR tube, the spectrum shown in Figure 9b was obtained. The complexity of this spectrum is reminiscent of that exhibited (Figure 8b) by the hexafluorophosphate salt **1-H-PF₆**. Subsequently, addition of an excess of Et_3N (20 mol equiv.) to the same NMR tube, followed by spectroscopic analysis, resulted in the spectrum shown in Figure 9c, which is essentially the same as that illustrated in Figure 9a, except that there are additional peaks arising from the presence of $[\text{Et}_3\text{NH}]^+[\text{CF}_3\text{CO}_2]^-$ and an excess of Et_3N . These observations suggest that addition of $\text{CF}_3\text{CO}_2\text{D}$ to the amine **1** results in deuteration to give the trifluoroacetate salt **1-D-O₂CCF₃**, which aggregates in a manner similar to the hexafluorophosphate salt **1-H-PF₆**. Subsequent addition of Et_3N deprotonates the ammonium center, thus reversing, and subsequently preventing, any aggregation.

Temperature Effects. The temperature-dependent ^1H NMR spectra (400 MHz) of a 98:2 $\text{CD}_3\text{CN}/\text{D}_2\text{O}$ solution of **1-H-PF₆** show (Figure 10) how increasing the temperature of the sample simplifies significantly the spectroscopic behavior. At 358 K, the aromatic region of the spectrum is very similar to that obtained (Figure 8a) when analyzing a CD_3SOCD_3 solution of **1-H-PF₆** at room temperature. It seems reasonable to conclude, therefore,

(29) Despite studying space-filling molecular models of the different diastereoisomeric dimeric superstructures, it is difficult to produce a rationalization for which diastereoisomer should result in a greater shift for the signal associated with H_1 , and which for H_3 .

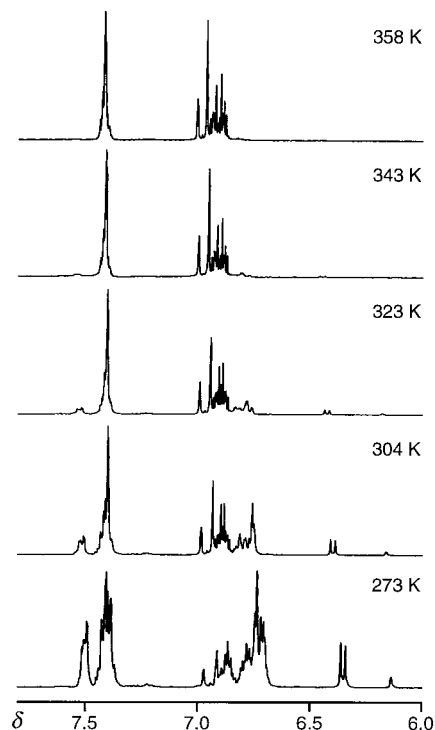


Figure 10. The temperature-dependent (273–358 K) partial ^1H NMR spectra of a $\text{CD}_3\text{CN}/\text{D}_2\text{O}$ (98:2) solution of **1-H-PF₆**.

that at 358 K in this $\text{CD}_3\text{CN}/\text{D}_2\text{O}$ mixture, there is negligible association of daisy chain monomers. However, as the temperature decreases, other signals in the spectrum, most notably the two upfield shifted doublets described above, start to 'grow', indicative of the formation of aggregated species. The lower the temperature becomes, the larger these peaks grow, a trend consistent with such a temperature-dependent assembly/disassembly. Simply put, in this particular system (with its own enthalpic and entropic nuances) the K_a value increases as the temperature decreases, resulting in a greater degree of aggregation at these lower temperatures.

Concentration Effects. To investigate its concentration dependent behavior, a 46.6 mmol CD_3CN solution of **1-H-PF₆** was prepared³⁰ and subjected to ^1H NMR spectroscopic analysis (400 MHz, 298 K). This solution was diluted repeatedly with known amounts of CD_3CN , and ^1H NMR spectra were recorded (partial region shown in Figure 11) at each particular concentration. As the solution becomes more and more dilute, eventually (at 0.026 mmol), the spectrum simplifies into one that is reminiscent of that obtained (Figure 8a) for a 10 mM solution of **1-H-PF₆** dissolved in CD_3SOCD_3 . In conclusion, therefore, at this very low monomer concentration, the only species present in solution is the free (non-aggregated) daisy chain monomer. At higher concentrations, however, the region from $\delta = 3.5$ – 4.3 ppm becomes ever more complicated, presumably as a result of the formation of aggregated species. Furthermore, at higher concentrations, signals clustered around $\delta = 4.7$ ppm—a chemical shift value that is characteristic of DB24C8-encircled NH_2^+ -adjacent benzylic methylene protons—begin to appear, thus suggesting the formation of inter-

(30) At concentrations greater than this one, **1-H-PF₆** begins to precipitate only a few minutes after complete dissolution.

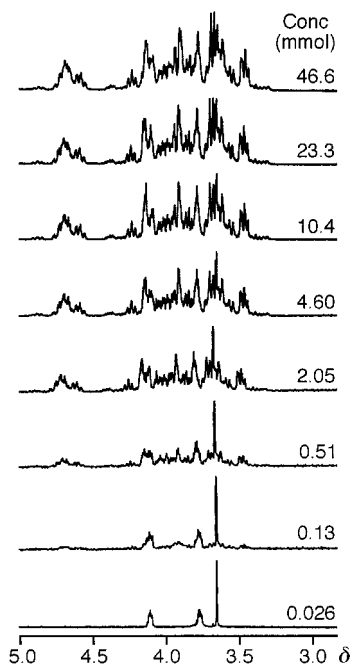


Figure 11. The concentration-dependent partial ^1H NMR spectra obtained from CD_3CN solutions of $\mathbf{1}\text{-H}\cdot\text{PF}_6$.

molecularly threaded aggregates, i.e., daisy chains. In addition, the characteristic *ortho*- and *meta*-coupled aromatic doublets (not shown) associated with dimer formation (vide supra) disappear at low concentration, but grow in intensity at higher concentrations. Despite these observations, however, little more can be said other than that $\mathbf{1}\text{-H}\cdot\text{PF}_6$, under the appropriate conditions of solvent polarity, concentration, and temperature, forms, reversibly, aggregated species that are presumed to have the threaded daisy chain architectures outlined in Figure 3.

A Deuterated Monomer. In an attempt to facilitate the interpretation of spectra obtained from this class of daisy chain compounds, $\mathbf{1}\text{-H}\cdot\text{PF}_6$ was 'resynthesized' using tetradeuterated catechol,³¹ giving rise to a compound ($\mathbf{11}\text{-H}\cdot\text{PF}_6$ in Figure 12) in which the most diagnostic resonances, those arising from H_1 , H_2 , and H_3 , are not obscured by other, less significant, ones.

Catechol- d_4 was synthesized³¹ from catechol using D_2SO_4 . Subsequently, the synthesis of the deuterium-masked daisy chain monomer $\mathbf{11}\text{-H}\cdot\text{PF}_6$ was carried out in the same manner as that which was employed in the synthesis of the parent (all ^1H) monomer.³² Subsequently, the ^1H NMR spectrum (400 MHz, 300 K) of $\mathbf{11}\text{-H}\cdot\text{PF}_6$ (20 mM) in CD_3CN revealed (Figure 12) the presence of *only* two different species in solution. As expected, the two characteristic upfield shifted doublets (*) are present. However, in this case, the corresponding signals for the appropriately coupled protons can be observed, for both major (‡) and minor (†) species, in the region from $\delta = 6.7\text{--}7.0$ ppm. This observation suggests that there are only two significant species in solution, which, based upon previous arguments, are likely to be the chiral and *meso* [*c2*]daisy chains (Figure 7).

(31) Baban, J. A.; Goodchild, N. J.; Roberts, B. P. *J. Chem. Soc., Perkin Trans. 2* **1986**, 157–161.

(32) The extent to which the catechol ring had been deuterated—93% of all catechol ^1H atoms were replaced by ^2H atoms—was calculated based upon the integrals observed in the ^1H NMR spectrum of the intermediate d_4 -formyl-substituted macrocycle **13**.

Two Fluorinated Monomers. We have witnessed previously how atom-substitution was used to mask a spectral response for this daisy chain system. Now, however, the use of fluorine atom labeling, to provide an additional spectroscopic probe via which a greater understanding of the solution-phase behavior of this system could be achieved, is described. The reason for placing fluorine atoms judiciously at strategic locations in the daisy chain monomer was to permit ^{19}F NMR spectroscopy to be employed in the solution-phase analysis of these systems. Whereas the resonances of numerous different protons in the structure would give rise, upon complexation, to many different signals in the ^1H NMR spectrum, one, or maybe two, fluorine atoms located in the structure, would be expected to give a simpler, and hence interpretable, ^{19}F NMR spectroscopic response.

***p*-F Systems.** To test the viability of this fluorine substitution strategy, a model system was first of all investigated. Bis(4-fluorobenzyl)ammonium hexafluorophosphate ($\mathbf{14}\text{-H}\cdot\text{PF}_6$) was prepared from commercially available starting materials. The binding of this F-substituted dibenzylammonium salt by DB24C8 (**2**) was then investigated, in the usual manner, by recording a ^1H NMR spectrum (400 MHz, 300 K) of a 1:1 mixture of the two components dissolved in CD_3CN . Subsequently, the K_a value for the association of $\mathbf{14}\text{-H}\cdot\text{PF}_6$ and DB24C8 at 300 K was calculated, using the single point method,³³ to be 875 M^{-1} . Gratifyingly, the ^{19}F NMR spectrum (376 MHz, 300 K) revealed the presence of two aromatic F peaks, separated by $\delta \sim 0.9$ ppm, corresponding to (i) 'free' $\mathbf{14}\text{-H}\cdot\text{PF}_6$, and (ii) bound $\mathbf{14}\text{-H}\cdot\text{PF}_6$, which, when integrated, gave values that resulted in the calculation of a K_a value exactly the same (875 M^{-1}) as that already determined using the ^1H NMR spectrum. This result prompted the synthesis of a fluoro-labeled daisy chain monomer, namely $\mathbf{17}\text{-H}\cdot\text{PF}_6$, in which the terminal phenyl ring carries a fluorine atom in the *para* position, in the hope that ^{19}F NMR spectroscopic analysis would prove much more enlightening than had previous ^1H NMR spectroscopic investigations on the unlabeled analogue.

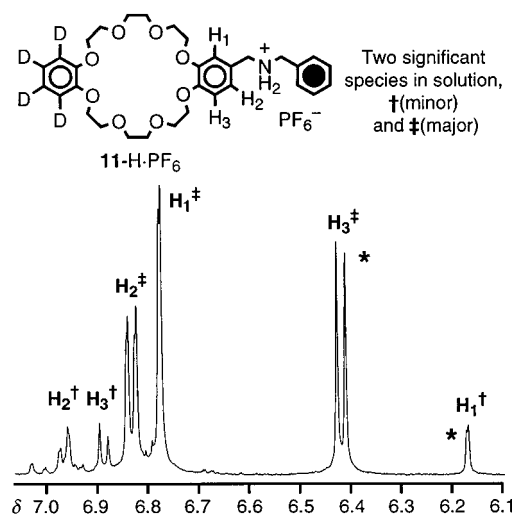
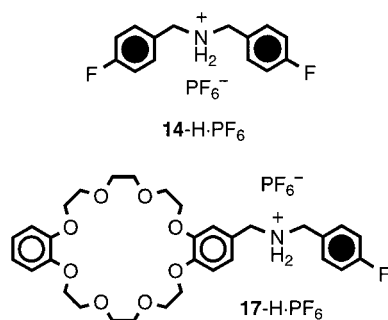


Figure 12. The partial ^1H NMR spectrum (400 MHz, 300 K) of a CD_3CN solution of the deuterium-labeled daisy chain monomer $\mathbf{11}\text{-H}\cdot\text{PF}_6$. Two sets (‡ and †) of signals are observed for the resonances of the protons (H_1 , H_2 , and H_3) of the central aromatic ring.



The synthesis of **17-H**·PF₆ began with the common CHO-substituted macrocycle precursor **9**. In the standard way, imine formation (with 4-fluorobenzylamine) was followed by (i) reduction, (ii) protonation, and finally, (iii) counterion exchange to afford the F-substituted daisy chain monomer **17-H**·PF₆ in very good yield. Except for variations in the aromatic region, as a consequence of the AA'BB' spin system of the terminal *p*-F substituted phenyl ring, the ¹H NMR spectrum of a 10 mM solution of **17-H**·PF₆ dissolved in CD₃CN was reminiscent of that obtained for the unsubstituted parent daisy chain monomer. Despite the complexity of the ¹H NMR spectrum, however, the ¹⁹F NMR spectrum contained (Figure 13, bottom) only three peaks (A, B, and C) that corresponded to the resonances of aromatic F atoms. In an effort to assign these peaks to either complexed or uncomplexed species, a 10 mM CD₃SOCD₃ solution of **17-H**·PF₆ was added portionwise to the original CD₃CN sample, and ¹H and ¹⁹F NMR spectra were recorded after each addition.³⁴ As the percentage CD₃SOCD₃ content of the CD₃CN solution of **17-H**·PF₆ increases (Figure 13), the peaks B and C begin to reduce in intensity as signal A grows in intensity. Ultimately, when just over 9% of the solvent mixture is CD₃SOCD₃, only one peak (A) remains. The corresponding ¹H NMR spectrum of this sample reveals that **17-H**·PF₆ is present only in the monomeric form under these conditions—as indicated by the simple nature of the spectrum. These experiments lead to the conclusion that peaks B and C arise as a consequence of aggregated species, i.e., daisy chains. In CD₃CN, ammonium ion binding is favorable and intermolecular association occurs, resulting in the formation of species that give rise to signals B and C). However, as the solvent polarity is

(33) In a slowly equilibrating complexation/decomplexation scenario, K_a values are determined as follows: integration of the peaks in the ¹H NMR spectrum associated with (1) free host, (2) free guest, and (3) 1:1 complex are measured, and by knowing accurately the concentrations of host and guest species that were dissolved initially, equilibrium concentrations can be determined. The K_a value is then given simply by dividing the equilibrium concentration of the 1:1 complex by the product of the equilibrium concentrations of the free host and guest species. To minimize errors in this study, numerous probe protons, associated with each of the three species present in solution, were used to calculate K_a values in any one spectrum. These K_a values were simply averaged for each spectrum. Furthermore, at least three independent ¹H NMR spectroscopic analyses were performed for each host:guest system, and the subsequent K_a values were once again averaged. For leading references on this method, see: Adrian, J. C.; Wilcox, C. S. *J. Am. Chem. Soc.* **1991**, *113*, 678–680.

(34) This experiment, therefore, allowed the change in solution-phase behavior to be monitored as the polarity of the solvent system was gradually increased. It is important to note, however, that in this process the sample is not diluted: since the CD₃SOCD₃ solution contains a 10 mM concentration of **17-H**·PF₆, the resulting solutions always maintain a 10 mM concentration of daisy chain monomer despite changes in volume. This fact is important, as now changes in the species present in solution, as monitored spectroscopically, can be attributed solely to solvent polarity, rather than to concentration effects.

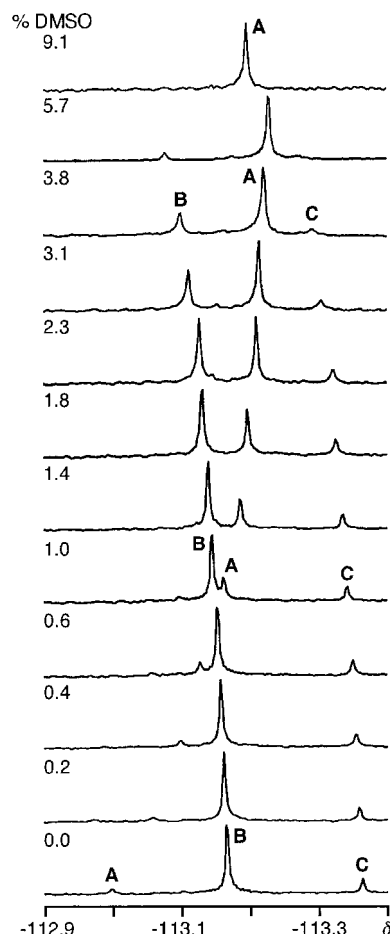


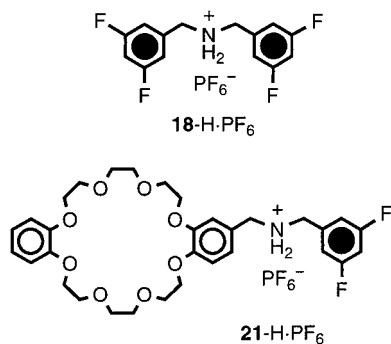
Figure 13. The partial ¹⁹F NMR spectra (376 MHz, 300 K) of a 10 mM solution of **17-H**·PF₆ dissolved in varying mixtures of CD₃CN/CD₃SOCD₃.

increased upon addition of CD₃SOCD₃, the NH₂⁺ sites become solvated by these solvent molecules, resulting in the deaggregation of daisy chains to form monomer, i.e., the species responsible for signal A. Furthermore, the presence of only two different aggregated species is in agreement with the behavior observed for the parent daisy chain systems (vide supra). Coincidentally, the ratio of peaks B and C is ~5:1, the same proportion as that observed for the two upfield shifted aromatic doublets which are so distinctive in the ¹H NMR spectra of both this analogue and the parent system. It seems reasonable, therefore, to propose that the two signals B and C, observed in the ¹⁹F NMR spectrum under aggregation-promoting conditions, originate from the two diastereoisomerically different [c2]daisy chains.³⁵

3,5-F₂ Systems. When located in the *para* position of the terminal phenyl ring, the F atom occupies a position that is as far away from the recognition site (the NH₂⁺ center) as possible. By placing F atoms in each of the

(35) This conclusion finds further support insofar as the presence of significant amounts of acyclic daisy chains, which would give rise to different patterns in the ¹⁹F NMR spectrum to those that are observed, can be ruled out. For example, in the case of the [a2]daisy chain, each F-atom lies in a different chemical environment, thus potentially resulting in two equal intensity peaks appearing in the spectrum. Upon the basis of the model two-component system (vide supra) in which 'free' and bound F-containing threadlike molecules give rise to signals ~0.9 ppm apart, it is unlikely that the resonances of the two different F atoms in the acyclic dimer would be isochronous. Obviously, a linear trimer would have F atoms occupying three different F environments, and so on.

meta positions, it was hoped that the influence of binding upon the environment of a fluorine substituent would be increased, resulting in a greater separation in the chemical shifts of the signals arising from the resonances of the F atoms attached to the 'free' and bound species, respectively. Therefore, the initial aim was to study a model system employing this substitution pattern—namely, bis(3,5-difluorobenzyl)ammonium hexafluorophosphate (**18**-H·PF₆). This salt was prepared starting from 3,5-difluorobenzaldehyde and 3,5-difluorobenzylamine. Imine formation, using a Dean-Stark apparatus to trap water generated during the reaction, followed by borohydride reduction, protonation, and counterion exchange, gave the desired F-labeled compound in very good yield. The binding of this F-substituted dibenzylammonium salt by DB24C8 (**2**) was then investigated, in the usual manner, by recording a ¹H NMR spectrum (400 MHz, 300 K) of a 1:1 mixture of the two components dissolved in CDCl₃/CD₃CN (3:1). Initially, the spectrum exhibited only peaks for each of the two free species, as if it was simply an overlay of the spectra of the two independent compounds, indicating that no complexation had occurred. Over a matter of weeks, however, **18**-H⁺ was observed to slowly thread through the cavity of DB24C8 to generate the corresponding [2]pseudorotaxane.³⁶



The synthesis of the 3,5-difluorophenyl-substituted [24]crown-8 based daisy chain monomer **21**-H·PF₆ began with the common formyl-substituted macrocycle precursor **9**. In the standard fashion, imine formation was followed by (i) reduction, (ii) protonation, and finally, (iii) counterion exchange. Once again, the initial spectroscopic

(36) ¹H NMR spectra were recorded over subsequent weeks, revealing the formation of a complex, albeit very slowly. The diagnostic multiplet at $\delta = 4.6$ increased in intensity with time while the ratio of 'free':bound thread can be most easily followed by monitoring the signals arising from the resonances of the γ protons of 'free' and bound DB24C8. Unfortunately, however, careful inspection of the corresponding ¹⁹F NMR spectra revealed that the sample was undergoing decomposition during the course of the analysis. Although more and more of the cation was slowly finding its way into DB24C8 macrocycles, the PF₆⁻ anion was, after ~100 h, no longer present. Interestingly, a new doublet, shifted upfield from the PF₆⁻ doublet by ~12 ppm, appears and then fades away with time as well. One possible explanation lies in the decomposition of PF₆⁻ to give PF₅, which, with a boiling point of -75 °C, although initially dissolved in solution, is drawn into the partial vacuum above the liquid that is formed upon sealing the NMR tube. Therefore, even although the system appears to be undergoing equilibration, the uncertainty surrounding the identity of the corresponding anion ended the experiment abruptly and prematurely. Nonetheless, the synthesis of the corresponding 3,5-F₂-substituted daisy chain monomer was undertaken, safe in the knowledge that, although slow in their passage, 3,5-F₂-substituted phenyl rings will pass through the macrocyclic cavity of DB24C8. Furthermore, the slow kinetics of threading/unthreading did not necessarily constitute a problem since they could potentially provide an opportunity to follow the assembly of daisy chain species on the human, rather than the NMR, time scale.

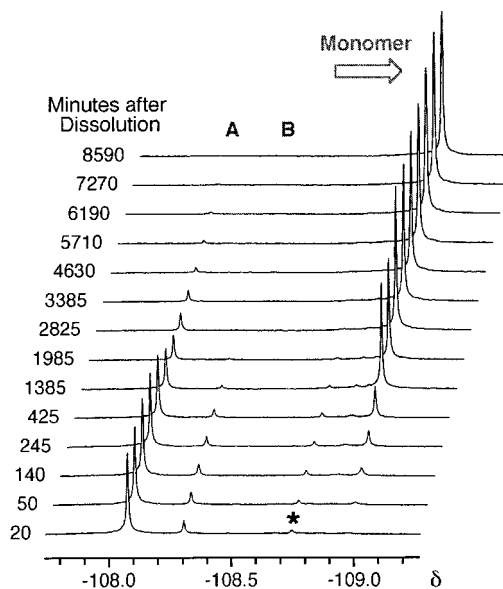


Figure 14. Partial ¹⁹F NMR spectra (376 MHz, 300 K) recorded over time of a CD₃SOCD₃ solution of **21**-H·PF₆.

analysis was performed in CD₃SOCD₃ in an effort to determine whether the compound was pure, i.e., since aggregation does not occur in this solvent, the purity of the sample can be assessed rather easily. Therefore, the ¹H NMR (400 MHz, 300 K) spectrum of **21**-H·PF₆ was greeted with some surprise. Instead of a simple spectrum, representing only the daisy chain monomer, a spectrum reminiscent of that obtained (recall Figure 8b) when a self-complementary daisy chain monomer is dissolved in aggregation-promoting CD₃CN was observed. Not only were the peaks in the aliphatic region smeared out across a wide chemical shift range, but the two distinctive upfield-shifted aromatic doublets (assigned up to now as arising from [c2]daisy chains) were also present. Furthermore, the ¹⁹F NMR spectrum (vide infra) contained more than one aromatic ¹⁹F peak, which is all that should be expected if the monomeric species is the only one present in solution. Not only was this initial spectrum a surprise but it was also transient! Upon rerunning the spectrum the next day, both the ¹H and ¹⁹F NMR spectra had changed significantly. This observation prompted a more in-depth analysis of this compound—one in which a sample of **21**-H·PF₆ was dissolved in CD₃SOCD₃ and monitored spectroscopically at more frequent intervals. The ¹⁹F NMR spectra recorded over a period of 6 d revealed (Figure 14) that, although initially two peaks (A and B) are present in the spectrum, eventually these signals disappear and give rise to one singlet, which, upon inspection of the corresponding simple ¹H NMR spectrum, can be assigned to a monomeric species. Therefore, it appears that **21**-H·PF₆ was isolated as a mixture of two aggregated daisy chain species, one giving rise to signal A, and the other, signal B, which, upon dissolution in CD₃SOCD₃, dissociate extremely slowly to give the daisy chain monomer.

Although complicated, the initial ¹H NMR spectrum contains the two diagnostic upfield shifted aromatic doublets that are indicative (vide supra) of the formation of the two possible diastereoisomeric [c2]daisy chains. Furthermore, the ¹⁹F NMR spectrum contains, initially, two signals (A and B), with an intensity ratio of ~5:1—a feature which is reminiscent of that observed for the *p*-F

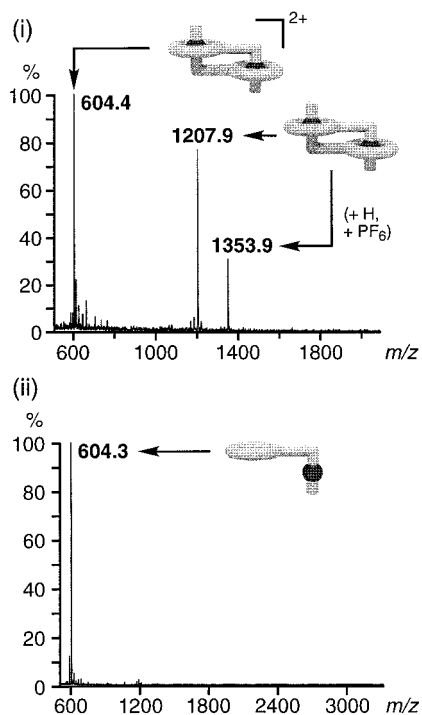


Figure 15. The FAB-mass spectra of **21**-H-PF₆ (i) prior to dissolution in CD₃SOCD₃, and (ii) after sitting in CD₃SOCD₃ solution for 6 d.

daisy chain system (**17**-H-PF₆). This observation suggests that there are *two different* F atom environments arising from *two different* F-containing aggregated species. Upon the basis of all of the evidence to hand, it is reasonable to conclude that these two aggregated species are indeed the two diastereoisomeric [*c2*]daisy chains. This conclusion is further supported by FAB mass spectrometric investigations that were subsequently performed on this compound. The FAB mass spectrum of the isolated solid, i.e., prior to dissolution in CD₃SOCD₃, reveals (Figure 15i) the presence of dimeric species. The signals at *m/z* values of 1207.9 and 1353.9, respectively, correspond to unipositive dimeric structures—the larger value arises as a consequence of an associated PF₆⁻ anion. Furthermore, the cluster of isotopic peaks centered around *m/z* = 604.4, are spaced by 0.5 mass units, indicating the presence of the doubly charged dimeric superstructure. This result suggests that no higher order daisy chain oligomers (i.e., trimers, tetramers, etc.) are to be found in the isolated sample, and that it consists solely of dimeric superstructures, of which there are only three: (i) the *two* diastereoisomeric [*c2*]daisy chains and (ii) the linear [*a2*]daisy chain. The second of these possibilities can be excluded based upon the simplicity (only two peaks, A and B in a ratio of ca. 5:1) of the initial ¹⁹F NMR spectrum. The reason is that, such an unsymmetric species would give rise to two equal intensity singlets, one each for a bound 3,5-difluorophenyl ring, and an unbound one—the same argument that was applied in explaining the ¹⁹F NMR spectra observed in the case of the *p*-F daisy chain system **17**-H-PF₆. Subsequently, the proposed composition of the six-day old CD₃SOCD₃ solution of **21**-H-PF₆ was confirmed (Figure 15ii) following FAB mass spectrometric analysis of this solution. Only a single peak (at *m/z* = 604.3) is observed in the spectrum and, since the adjacent isotope peaks are separated by unity, only the monomeric daisy chain

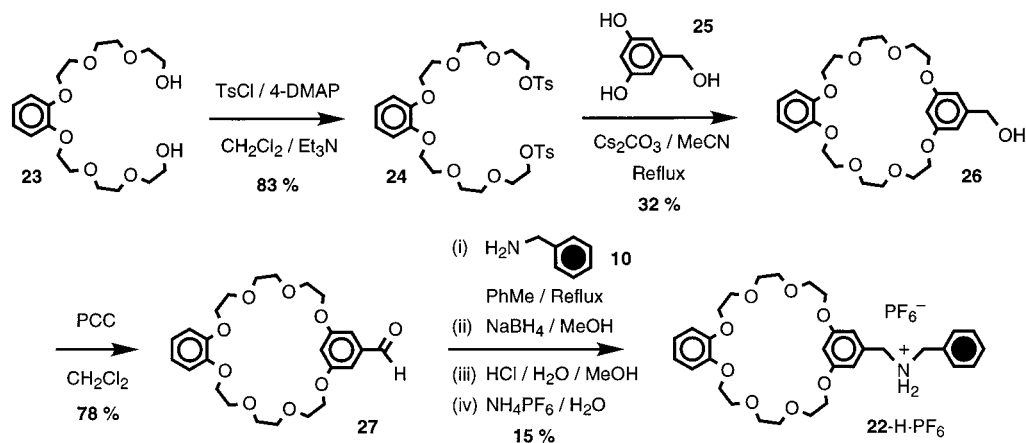
species remains, i.e., there are no longer any aggregated assemblies present.

There is, however, one feature of the spectra illustrated in Figure 14, that remains to be explained. A small signal (*) is evident at $\delta = -108.7$ ppm. Initially, it grows ever so slightly in intensity, and then 'shrinks back' into the baseline of the spectrum until it is no longer visible at the end of the experiment. Perhaps, finally, we are 'seeing' a little of the [*a2*]daisy chain. When the [*c2*]daisy chains dissociate to give the monomeric structure, unless both 3,5-difluorophenyl terminated arms dethread simultaneously, some of the [*a2*]daisy chain will inevitably be formed. Such a structure contains both 'free' and bound ammonium ion-containing arms, each of which is terminated by a 3,5-difluorophenyl group. The [*a2*]daisy chain would be expected to give rise to two equal intensity peaks in the ¹⁹F NMR spectrum. It is likely that the peak at $\delta = -108.7$ ppm corresponds to the resonance of the F atoms of the 'free' ammonium ion-containing arm of the [*a2*]daisy chain, while the corresponding signal for the bound arm remains hidden under either peak A or B. As the intensity of this peak never 'grows' to any significant proportions, such an explanation would require the rate constant for the transformation of [*c2*]daisy chain into [*a2*]daisy chain to be smaller than that for the conversion of [*a2*]daisy chain into [*a1*]daisy chain, i.e., the monomer. It is not unreasonable to propose that the more tangled nature of the cyclic superstructure, with less degrees of translational and rotational freedom, as compared with the linear [*a2*]daisy chain superstructure, may offer an explanation for this observation. At this point, therefore, there is no doubt regarding the absence of higher order daisy chain superstructures in the initial solution. For example, the presence of a [*c3*]daisy chain would, in the process of its CD₃SOCD₃-induced dismemberment, generate [*a2*]- and [*a3*]daisy chains (the latter complex having *three* distinct F atom environments), almost certainly giving rise to a more complicated set of spectra than those observed experimentally. Obviously the situation would be considerably more complicated for even larger daisy chain complexes.

[25]Crown-8-Based Systems. It is clear that gaining an appreciation of the aggregation behavior of [24]crown-8 based daisy chain systems is hampered by the formation of stereoisomeric superstructures. In an effort to remove this stereochemical ambiguity, monomers based upon a [25]crown-8 macrocycle were investigated as candidates for the formation of aggregated daisy chains. Although crown ethers with a [25]crown-8 constitution have been shown³⁷ to have much lower affinities for secondary ammonium ions than their DB24C8-based counterparts, the more highly symmetric nature of the prototypical [25]crown-8 daisy chain monomer (**22**-H-PF₆), as compared to the [24]crown-8 monomer (**1**-H-PF₆), means that, upon assembly, only one unique [*c2*]daisy chain is formed. Furthermore, only one form of each of the higher order aggregates, i.e., [*c3*]daisy chain, [*c4*]daisy chain, etc., is possible.

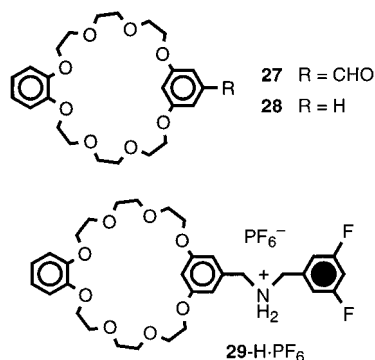
The Parent Monomer. The synthesis of this [25]-crown-8-based self-complementary daisy chain monomer is outlined in Scheme 2. Tosylation of the known³⁸ diol **23**, under standard conditions, gave the ditosylate **24**,

(37) Ashton, P. R.; Bartsch, R. A.; Cantrill, S. J.; Hanes, R. E., Jr.; Hickingbottom, S. K.; Lowe, J. N.; Preece, J. A.; Stoddart, J. F.; Talanov, V. S.; Wang, Z.-H. *Tetrahedron Lett.* **1999**, *40*, 3661–3664.

Scheme 2. The Synthesis of the Parent [25]Crown-8-Based Daisy-Chain Monomer **22**·H·PF₆

which was subsequently reacted with 3,5-dihydroxybenzyl alcohol (**25**) to give the hydroxymethyl-substituted BMP25C8 derivative **26** in reasonable yield. Oxidation of the hydroxyl group of **26** with PCC gave the corresponding formyl-substituted macrocycle **27** in good yield. Subsequent condensation of **27** with benzylamine (**10**), followed by borohydride reduction, protonation (HCl), and counterion exchange from Cl⁻ to PF₆⁻, afforded the target compound **22**·H·PF₆ in a 15% yield.

more amenable to analysis. Not only would a slowly exchanging system be preferable spectroscopically, but, as observed in the [24]crown-8 series, it was felt that a ¹⁹F probe might prove helpful. One candidate immediately sprang to mind – namely, the 3,5-difluorophenyl group, which had been shown to pass very slowly through a DB24C8 sized macrocycle. Might it also prove useful in the [25]crown-8-based system? Before proceeding with the synthesis of a 3,5-difluorophenyl terminated [25]crown-8 daisy chain monomer, the appropriate model system was investigated. A CD₃CN solution containing a 1:1 mixture of bis(3,5-difluorobenzyl)ammonium hexafluorophosphate (**18**·H·PF₆) and BMP25C8 (**28**) was subjected to both ¹H and ¹⁹F NMR spectroscopic analyses. The ¹H NMR spectrum was characteristic of a slowly exchanging crown ether/dibenzylammonium ion system. Signals were observed for all three species present in solution, namely (i) 'free' BMP25C8, (ii) 'free' **18**·H·PF₆, and (iii) the [2]pseudorotaxane [**28**·**18**·H]PF₆. Consequently, this spectrum was used to calculate, using the single point method³³, a *K_a* value (at 300 K in CD₃CN) of 25 M⁻¹ for the association of these two species. Furthermore, the ¹⁹F NMR spectrum revealed the presence of two aromatic F singlets, one each for the 'free' and bound bis(3,5-difluorobenzyl)ammonium cation. Crucially, the *K_a* value, when calculated based upon the intensities of these two peaks, was the same as that already obtained from the data extracted from the ¹H NMR spectrum. The slow passage, on the NMR time scale, of a 3,5-difluorophenyl ring through the cavity of BMP25C8 prompted the synthesis of the correspondingly substituted daisy chain analogue, namely **29**·H·PF₆.



Unlike the [24]crown-8 daisy chain analogues, **22**·H·PF₆ was found to be soluble in CD₂Cl₂, perhaps the optimal solvent²⁵ for the crown ether/ammonium ion interaction, and, therefore, subsequent ¹H NMR investigations were conducted in this solvent. Unfortunately, as expected,^{18j,37} the kinetics associated with the threading/dethreading of a phenyl ring through a [25]crown-8 sized macrocycle are such that neither a slow- nor a fast-exchange regime operates. Consequently, ¹H NMR spectra obtained from solutions of **22**·H·PF₆ over a range (0.05–28.5 mM) of concentrations consist of broad peaks that are difficult to assign to any particular species. The spectroscopic changes observed over a given concentration range indicate that aggregation, to some extent, does occur with this [25]crown-8-based monomer. Furthermore, the FAB mass spectrum of **22**·H·PF₆ contains a peak, albeit very small (ca. 3% of the peak arising from the monomer), corresponding to a dimeric assembly.

A Fluorinated Monomer. The limited information garnered from the study of the parent [25]crown-8 daisy chain prompted the search for a system that would be

The synthesis of **29**·H·PF₆ started from the formyl-substituted macrocycle precursor **27**. In standard fashion, imine formation (with 3,5-difluorobenzylamine) was followed by (i) reduction, (ii) protonation, and finally, (iii) counterion exchange, to afford the 3,5-difluorophenyl-substituted daisy chain monomer **29**·H·PF₆ in a 17% yield. The initial ¹H and ¹⁹F NMR spectroscopic characterization, which was carried out in CD₃SOCD₃, revealed the daisy chain monomer to be pure: a simple, easily assignable, ¹H NMR spectrum was obtained, and the ¹⁹F NMR spectrum contained a single peak corresponding to the aromatic F atoms, in addition to the doublet for the PF₆⁻ anion. Mass spectrometry (FAB) revealed the formation, in the 'gas phase', of dimeric superstructures, as evidenced by the presence of signals corresponding to both the uni- and dipositive dimers. More interesting,

(38) Mertens, I. J. A.; Wegh, R.; Jennekens, L. W.; Vlietstra, E. J.; van der Kerk-van Hoof, A.; Zwikker, J. W.; Cleij, T. J.; Smeets, W. J. J.; Veldman, N.; Spek, A. L. *J. Chem. Soc., Perkin Trans. 2* **1998**, 725–735.

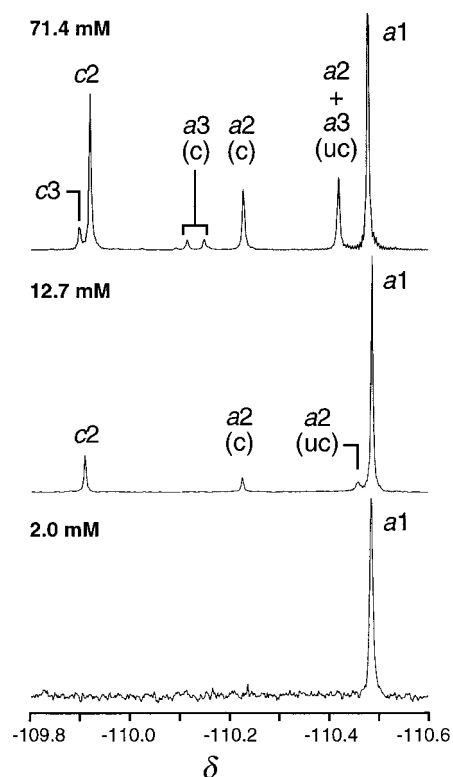


Figure 16. The concentration-dependent partial ^{19}F NMR spectra (376 MHz, 298 K, CD_3CN) of $\mathbf{29}\cdot\text{H}\cdot\text{PF}_6$.

however, were the concentration-dependent ^{19}F NMR spectroscopic investigations conducted³⁹ in CD_3CN solution.

The ^{19}F NMR spectra obtained from three samples containing different concentrations of $\mathbf{29}\cdot\text{H}\cdot\text{PF}_6$ (2.0, 12.7, and 71.4 mM, respectively) revealed (Figure 16) a dramatic concentration dependence. The least concentrated sample (2.0 mM) gave rise to a ^{19}F NMR spectrum containing a single aromatic F signal. Inspection of the corresponding ^1H NMR spectrum, which was reminiscent of that obtained when $\mathbf{29}\cdot\text{H}\cdot\text{PF}_6$ was dissolved in CD_3SOCD_3 , confirmed that the single F resonance could be attributed to the monomeric species, i.e., the [a1]daisy chain. The ^{19}F NMR spectrum arising from the sample of intermediate concentration (12.7 mM) contained three additional aromatic F signals. From these extra peaks, it can be inferred that, at this higher concentration, intermolecular aggregation is starting to occur and results in the formation of new species. The presence of two small equal-intensity peaks ($\delta = -110.46$ and -110.22 , respectively) suggest the presence of an [a2]daisy chain in which one of the 3,5-difluorophenyl-terminated ammonium ion-containing arms is complexed, and the other one is not. One peak has a chemical shift similar to that observed for the monomeric species, whereas the other one is shifted downfield, consistent with complex formation, as was observed in the case of the model $\text{BMP25C8}/\mathbf{18}\cdot\text{H}\cdot\text{PF}_6$ system. Even further downfield shifted is another singlet ($\delta = -109.90$), which, most likely, corresponds to the [c2]daisy chain in which all of the F atoms reside in equivalent environments. The ^{19}F NMR spectrum, obtained from the most concentrated

sample (71.4 mM) investigated in this study, is, appropriately, the most complicated. At this concentration, a new peak is observed to appear just downfield of that assigned to the [c2]daisy chain, and can, therefore, be attributed to the [c3]daisy chain. Correspondingly, peaks that can be attributed to the acyclic trimer ([a3]daisy chain) are also annotated on the spectrum. Two small equal-intensity peaks ($\delta = -110.12$ and -110.15 , respectively) are observed in the same region of the spectrum as the peak ($\delta = -110.22$) corresponding to the resonance of the F atoms on the complexed arm of the [a2]daisy chain. The [a3]daisy chain is expected (Figure 17) to give rise to three equal intensity signals, two corresponding to the F atom resonances of bound arms and one arising from the resonance of the F atoms in the 'free' arm. It is not unreasonable to propose that the peak associated with this latter resonance overlaps with the peak arising from the corresponding resonance of the 'free' arm of the [a2]daisy chain. This hypothesis gains further support when it is considered that the signal labeled 'a2 + a3 (uc)' has an intensity equal to the sum of the intensities of the peak corresponding to a2 (c) and one of the a3 (c) peaks. Although these assignments cannot be made with absolute certainty, they are consistent with (i) the anticipated solution phase behavior, upon increasing concentration, of an aggregating self-complementary system, (ii) the number and intensity ratios of peaks that would be expected to arise from the proposed species, as well as (iii) the relative chemical shift values that would arise for peaks corresponding to the resonances of either 'free' or bound F-containing arms. Assuming the correct interpretation of the spectrum, K_a values for the appropriate assembly steps (recall Figure 3) were calculated, employing the single point method, based upon the data contained with the ^{19}F NMR spectrum obtained from the 71.4 mM sample. Although the values obtained ($K_{a2} = 8.2 \text{ M}^{-1}$; $K_{c2} = 1.2$; $K_{a3} = 6.5 \text{ M}^{-1}$; $K_{c3} = 0.7$) are lower

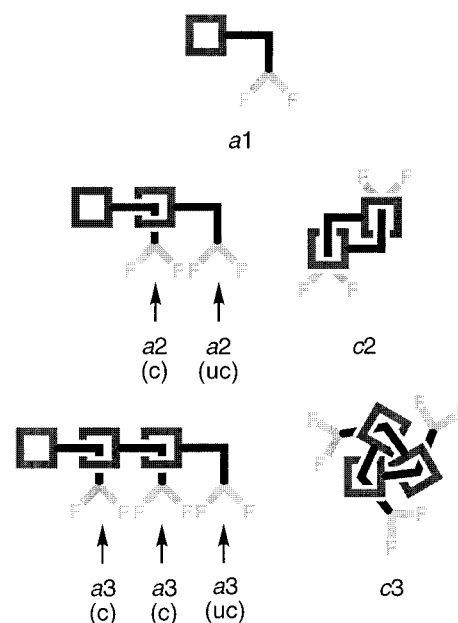


Figure 17. A schematic representation depicting the 'free' and bound ammonium ion-containing arms of aggregated (up to, and including, trimeric) daisy chain superstructures.

(39) The solvent of choice was CD_3CN , as no meaningful ^1H or ^{19}F NMR spectroscopic results were obtained for CD_3NO_2 or CD_2Cl_2 solutions of $\mathbf{29}\cdot\text{H}\cdot\text{PF}_6$.

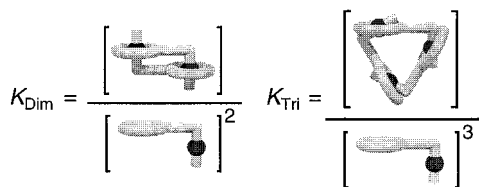


Figure 18. Expressions for the overall cyclic dimerization and trimerization constants in a self-complementary daisy-chain system.

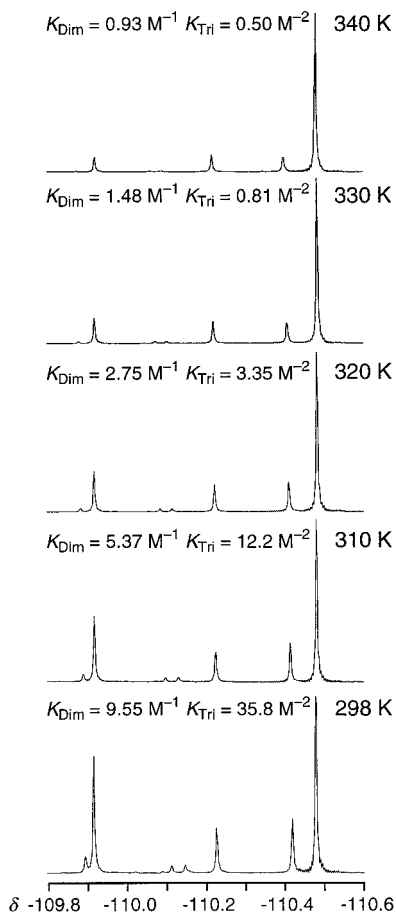


Figure 19. The temperature-dependent partial ^{19}F NMR spectra (376 MHz, CD_3CN) of $29\text{-H}\cdot\text{PF}_6$.

than those observed for the model system ($K_a = 25 \text{ M}^{-1}$), this outcome is not unexpected.⁴⁰

For such a self-assembling system, it is possible to define (Figure 18) *overall* cyclic dimerization and cyclic trimerization constants, namely K_{Dim} and K_{Tri} , respectively. By utilizing variable temperature ^{19}F NMR spectroscopy (Figure 19), values for these association constants were calculated at different temperatures. An increase in the temperature of the solution resulted in a decrease in the amount of dimeric and trimeric species observed. Such a trend is reflected in the ever-decreasing values of K_{Dim} and K_{Tri} as the temperature rises. By constructing a van't Hoff plot for each of these species

(40) The lower values of K_a than those observed in the model system may reflect the fact that oligomerization of this self-complementary system always requires bringing together two positively charged species. This repulsive Coulombic effect may serve to reduce the overall affinity for two daisy chain monomers in comparison with the model two-component system, in which a *cationic* thread is bound by a *neutral* macrocycle.

(Figure 20), the enthalpic and entropic contributions to the formation of these species can be determined. Straight lines, each with a good fit, can be approximated to the experimental data, revealing that (i) the formation of the $[\text{c}3]$ daisy chain is more *enthalpically* favorable than the assembly of the $[\text{c}2]$ daisy chain, whereas (ii) entropy factors favor the formation of the cyclic dimeric, rather than the trimeric, superstructure. These results are not unexpected: assembly of the $[\text{c}3]$ daisy chain proceeds with the creation of more noncovalent interactions than does the formation of the $[\text{c}2]$ daisy chain, but it requires the assembly of three separate components rather than two. One important point to note is that the enthalpic gain upon cyclic trimerization is almost twice as much as that calculated for cyclic dimerization. Upon the basis of the fact that the formation of a $[\text{c}3]$ daisy chain results from three crown ether/ammonium ion interactions, and two such interactions are responsible for $[\text{c}2]$ daisy chain formation, why do the enthalpic terms not reflect this 3:2 ratio? Furthermore, in the case of the $[\text{24}]$ crown-8 daisy chains, the stacking of the central aromatic rings appears to account for a significant stabilization of the $[\text{c}2]$ superstructure, resulting in their domination of both the solution- and solid-state properties. If extrapolated to the $[\text{25}]$ crown-8-based systems, this additional π - π derived stabilization would surely result in an even smaller ratio of the enthalpy changes observed for cyclic trimerization versus dimerization. Perhaps the fact that such an effect is not observed, means that, in the $[\text{25}]$ crown-8 series the $[\text{c}2]$ superstructure does not represent such an island of stability as it does in the case of the $[\text{24}]$ crown-8 analogues. In retrospect, this observation is also reflected in the values of K_{a2} and K_{c2} obtained for $29\text{-H}\cdot\text{PF}_6$. Whereas K_{a2} is over six times larger than K_{c2} in the $[\text{25}]$ crown-8 series, the trend, if not the magnitude, is believed to be reversed in the $[\text{24}]$ crown-8 series.²¹

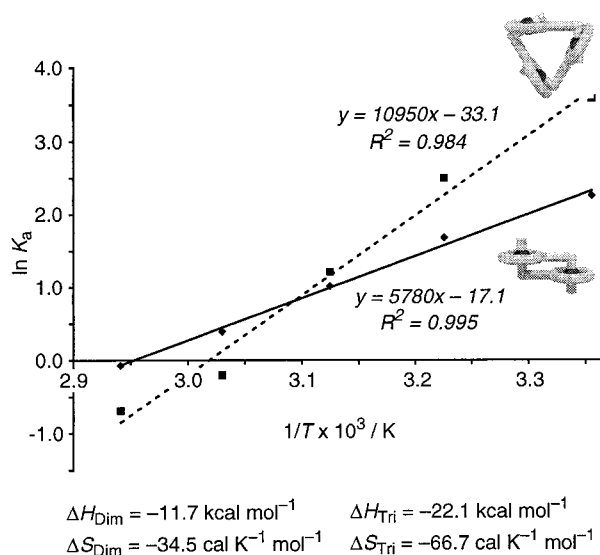


Figure 20. The van't Hoff plot obtained upon plotting $\ln K_a$ vs $1/T$ for the K_a values determined from the partial ^{19}F NMR spectra illustrated in Figure 19.

Conclusions

It has been shown that self-complementary dibenzyl-ammonium ion substituted crown ethers, with either a $[\text{24}]$ - or $[\text{25}]$ crown-8 constitution, will aggregate to give daisy chain assemblies under the appropriate conditions

of concentration, temperature, and solvent polarity. These supramolecular aggregates, however, fall far short of the suprapolymeric systems described in the Introduction of this paper. Although intramolecular self-complexation is not an option for these daisy chain molecules, a growing chain quickly finds its own tail and cyclizes, preventing any further chain propagation. In the case of the [24]crown-8 systems, there is overwhelming evidence to suggest that, over a wide concentration range, the [c2]daisy chain is by far the most favorable assembly. This conclusion was not reached easily or lightly. It required the application of deuterium- as well as fluorine-labeling, in conjunction with extensive concentration- and temperature-dependent spectroscopic studies. Furthermore, the interpretation of the spectroscopic data collected for these compounds is complicated by the formation of stereoisomeric aggregates. In an attempt to alleviate this subtle stereochemical nuance, more symmetrical daisy chain monomers based upon [25]crown-8 macrocycles were prepared and studied. Not only is the spectroscopic behavior of these modified daisy chain monomers considerably simpler, but the [c2]daisy chain superstructure no longer represents a dead-end for chain growth. The weaker interaction between secondary dialkylammonium ions and [25]crown-8-based macrocycles, however, undermines the effectiveness of this supramolecular system. Although trimeric aggregates are observed in solution, these species are not predicted to rise to significant levels at concentrations < 1 M. Consequently, the concentration at which a species considered to be supramolecular polymer would be formed is likely to far exceed the solubility limits of these salts. In summary, although not precursors for interwoven supramolecular polymers, the compounds reported in this paper represent interesting examples of interwoven supermolecules that could be utilized, with appropriate modification, in the formation of mechanically interlocked polymers.

Experimental Section

General. Chemicals were purchased from Aldrich and Lancaster Synthesis Ltd and used as received unless indicated otherwise. Compounds **12**³¹ and **23**³⁸ were prepared according to literature procedures. The synthesis and characterization data for BMP25C8 (**28**) have been reported elsewhere.^{18j} Solvents were dried according to literature procedures.⁴¹ Thin-layer chromatography was carried out using aluminum sheets precoated with silica gel 60F (Merck 5554). The plates were inspected by UV light and, if required, developed in I₂ vapor. Column chromatography was carried out using silica gel 60F (Merck 9385, 0.040–0.063 mm). Melting points were determined on an Electrothermal 9100 apparatus and are uncorrected. ¹H and ¹³C NMR spectra were recorded on either a Bruker AC300 (300 and 75 MHz, respectively), Bruker ARX400 (400 and 100 MHz, respectively), or Bruker ARX500 (500 and 125 MHz, respectively) spectrometer, using residual solvent as the internal standard. ¹H-Decoupled ¹⁹F NMR spectra were recorded on a Bruker ARX400 (376 MHz) spectrometer and were referenced to C₆F₆ (−163.0 ppm) present as a CH₂Cl₂ solution in an internal capillary tube. All chemical shifts are quoted on the δ scale, and all coupling constants are expressed in hertz (Hz). Liquid secondary ion (LSI) mass spectra were obtained on a VG Zabspec mass spectrometer, equipped with a cesium ion source and utilizing a *m*-nitrobenzyl alcohol matrix. Fast atom bombardment (FAB) mass spectra were obtained using a ZAB-SE mass spectrometer, equipped with

a krypton primary atom beam, utilizing a *m*-nitrobenzyl alcohol matrix. Cesium iodide or poly(ethylene glycol) was employed as a reference compound. Electron impact mass spectra (EIMS) were obtained from a VG Prospec mass spectrometer. Microanalyses were performed by either the University of North London Microanalytical Service (UK) or Quantitative Technologies, Inc..

3,4-Bis{2-[2-(2-hydroxyethoxy)ethoxy]ethoxy}benzaldehyde (6). 3,4-Dihydroxybenzaldehyde (**4**) (15.1 g, 0.11 mol), K₂CO₃ (37.3 g, 0.27 mol), and LiBr (9.5 g, 0.11 mol) were placed in a 2 L round-bottomed flask fitted with a condenser and a pressure-equalized dropping funnel. The system was flushed with N₂, and anhydrous DMF (500 mL) was introduced into the flask. 2-[2-(2-Chloroethoxy)ethoxy]ethanol (**5**) (40.6 g, 0.24 mol) was dissolved in DMF (100 mL) and added to the dropping funnel, again through a flow of nitrogen. The suspension in the flask was heated to 100 °C while stirring, and the solution of **5** was added dropwise over 1 h. The reaction mixture was stirred at 100 °C for a further 3 d under a continuous flow of N₂. After this time, the reaction mixture was filtered (in order to remove inorganic salts) and evaporated to dryness, and the residue was partitioned between CH₂Cl₂ (300 mL) and 10% w/v K₂CO₃ solution (300 mL). The organic layer was further washed with 10% w/v K₂CO₃ solution (3 × 100 mL). The organic phase was dried (MgSO₄), and the solvents were removed in vacuo to yield **6** as a brown oil (39.1 g, 89%). This oil was used in subsequent reactions without further purification. An analytically pure sample was obtained as a pale yellow oil after chromatography (SiO₂: gradient elution with CH₂Cl₂/MeOH, 100:0 to 96:4); ¹H NMR (300 MHz, CDCl₃): δ = 3.32 (br s, 2H), 3.52–3.74 (m, 16H), 3.83–3.90 (m, 4H), 4.14–4.23 (m, 4H), 6.94 (d, *J* = 8.1 Hz, 1H), 7.35–7.42 (m, 2H), 9.77 (s, 1H); ¹³C NMR (75 MHz, CDCl₃): δ = 61.5, 68.5, 69.2, 69.3, 70.2, 70.7, 70.8, 72.6, 111.5, 112.2, 126.7, 130.1, 148.9, 154.0, 190.8; MS (EI): *m/z* (%): 402 (37) [*M*]⁺; C₁₉H₃₀O₉ (402.4): calcd C 56.71, H 7.51; found C 56.88, H 7.41.

3,4-Bis{2-[2-(*p*-toluenesulfonyloxy)ethoxy]ethoxy}benzaldehyde (7). Diol **6** (26.6 g, 66.0 mmol), Et₃N (66.8 g, 660 mmol) and a catalytic amount of 4-(dimethylamino)pyridine were dissolved in CH₂Cl₂ (400 mL), and this solution was stirred and cooled (0–5 °C). A solution of *p*-toluenesulfonyl chloride (62.9 g, 330 mmol) in CH₂Cl₂ (200 mL) was then added dropwise over a period of 3 h, maintaining the reaction temperature below 5 °C. Subsequently, the reaction mixture was allowed to warm to ambient temperature and left to stir for a further 8 h under a continuous flow of N₂. The reaction mixture was acidified with 5 M HCl solution (250 mL), and the organic layer was washed with 2 M HCl solution (200 mL) and saturated brine (2 × 200 mL). The organic layer was dried (MgSO₄), and the solvents were removed in vacuo. The residue was purified by column chromatography (SiO₂: gradient elution with EtOAc/C₆H₁₄, 50:50 to 80:20) to yield the desired compound **7** as a pale yellow oil (26.8 g, 57%); ¹H NMR (300 MHz, CDCl₃): δ = 2.38 (s, 6H), 3.53–3.67 (m, 12H), 3.78–3.86 (m, 4H), 4.08–4.21 (m, 8H), 6.96 (d, *J* = 8.1 Hz, 1H), 7.29 (d, *J* = 8.5 Hz, 4H), 7.36–7.43 (m, 2H), 7.74 (d, *J* = 8.5 Hz, 4H), 9.78 (s, 1H); ¹³C NMR (75 MHz, CDCl₃): δ = 21.8, 68.9, 69.4, 69.6, 69.7, 70.9, 71.5, 111.5, 112.0, 112.7, 126.9, 128.1, 130.0, 130.4, 133.1, 145.0, 149.3, 154.5, 191.0; MS (FAB): *m/z* (%): 711 (21) [*M*]⁺; C₁₉H₃₀O₉ (710.8): calcd C 55.76, H 5.96; found C 55.74, H 5.75.

(2-Formyl)dibenzo[24]crown-8 (9). Cesium carbonate (19.3 g, 59.3 mmol) was placed in a 1 L round-bottomed flask fitted with condenser and pressure-equalized dropping funnel. The system was flushed with N₂, and anhydrous DMF (200 mL) was added to the flask. The ditosylate **7** (8.43 g, 11.9 mmol) and catechol (**8**) (1.31 g, 11.9 mmol) were dissolved in DMF (500 mL) and added to the dropping funnel, again through a flow of N₂. The suspension in the flask was heated to 100 °C while stirring, and the ditosylate/catechol solution was added dropwise over 24 h. This mixture was stirred at 100 °C, under an N₂ atmosphere, for a further 7 d. Subsequently, the solvent was removed in vacuo and the residue partitioned between PhMe (300 mL) and 10% w/v K₂CO₃ solution (300 mL). The aqueous layer was further extracted

(41) Perrin, D. D.; Armarego, W. F. L. *Purification of Laboratory Chemicals*; Pergamon: Oxford, 1989.

with PhMe (3 × 200 mL), and the combined organic layers were washed with 10% w/v K₂CO₃ solution (300 mL). The organic phase was dried (MgSO₄), and the solvents were removed in vacuo. The residue was subjected to column chromatography (SiO₂: gradient elution with EtOAc/MeOH, 100:0 to 95:5) to yield an off-white solid which was recrystallized from EtOAc/C₆H₁₄ to yield the desired compound **9** as a white solid (2.31 g, 41%); mp 105–107 °C; ¹H NMR (300 MHz, CDCl₃): δ = 3.82–3.85 (m, 8H), 3.89–3.97 (m, 8H), 4.12–4.24 (m, 8H), 6.83–6.90 (m, 4H), 6.93 (d, *J* = 8.1 Hz, 1H), 7.37 (d, *J* = 1.8 Hz, 1H), 7.42 (dd, *J* = 1.8, 8.1 Hz, 2H), 9.81 (s, 1H); ¹³C NMR (75 MHz, CDCl₃): δ = 69.4, 69.5, 69.7, 70.0, 71.3, 71.4, 71.5, 111.1, 111.9, 114.0, 121.4, 126.8, 130.2, 148.9, 149.2, 154.3, 190.9; MS (FAB): *m/z* (%): 477 (100) [*M* + H]⁺, 494 (13) [*M* + NH₄]⁺, 499 (24) [*M* + Na]⁺, 515 (5) [*M* + K]⁺; C₂₅H₃₂O₉ (476.5): calcd C 63.01, H 6.77; found C 63.12, H 6.54.

(2-Benzylaminomethyl)dibenzo[24]crown-8 (1). A solution of the formyl crown ether **9** (1.50 g, 3.15 mmol) and benzylamine **10** (337 mg, 3.15 mmol) was heated under reflux for 30 h in PhMe (150 mL) using a Dean–Stark apparatus. When the reaction mixture had cooled to ambient temperature, an aliquot (ca. 1 mL) was removed, and the solvent was evaporated in vacuo to give a yellow oily residue which was shown by ¹H NMR to be the imine; ¹H NMR (300 MHz, CDCl₃): δ = 3.85–3.98 (m, 16H), 4.13–4.23 (m, 8H), 4.81 (s, 2H), 6.85–6.95 (m, 5H), 7.16–7.45 (m, 7H), 8.28 (s, 1H). The reaction mixture was diluted with dry MeOH (100 mL), and then NaBH₄ (1.19 g, 31.5 mmol) was added portionwise to the stirring solution over a period of 1 h. Stirring was maintained under ambient conditions for a further 24 h, after which time 5 M HCl solution (250 mL) was added to the reaction mixture. The solvents were removed in vacuo, and the residue was partitioned between 2 M NaOH solution (250 mL) and CH₂Cl₂ (250 mL). The aqueous layer was extracted with CH₂Cl₂ (2 × 100 mL), and the combined organic extracts were dried (MgSO₄). The solvents were removed in vacuo, yielding a crude product which was subjected to column chromatography (SiO₂: Me₂CO) to yield the title compound **1** as a pale yellow oil (1.42 g, 79%); ¹H NMR (300 MHz, CDCl₃): δ = 3.71 (s, 2H), 3.77 (s, 2H), 3.82 (s, 8H), 3.88–3.93 (m, 8H), 4.11–4.17 (m, 8H), 6.78–6.91 (m, 5H), 7.20–7.34 (m, 7H); ¹³C NMR (75 MHz, CDCl₃): δ = 52.9, 53.2, 69.5, 69.6, 70.0, 71.3, 114.0, 114.2, 121.0, 121.5, 127.0, 128.3, 128.5, 133.7, 140.4, 147.9, 149.0; MS (LSD): *m/z* (%): 568 (15) [*M* + H]⁺ and [2*M* + 2H]²⁺, 1135 (100) [2*M* + H]⁺; C₃₂H₄₁NO₈ (567.7): calcd C 67.71, H 7.28, N 2.47; found C 67.75, H 7.29, N 2.39.

(2-Benzylammoniummethyl)dibenzo[24]crown-8 Hexafluorophosphate (1-H·PF₆). Amine **1** (470 mg 0.83 mmol) was dissolved in 5 M HCl solution (50 mL), and the resulting solution was evaporated to dryness. The residue was dissolved in hot water (ca. 15 mL), and a saturated aqueous solution of NH₄PF₆ was added until no further precipitation occurred. The white precipitate was collected, washed with copious amounts of H₂O, and dried to yield the hexafluorophosphate salt **1-H·PF₆** as a white powder (552 mg, 93%); mp >210 °C (decomp); ¹H NMR (300 MHz, CD₃SOCD₃): δ = 3.68 (s, 8H), 3.74–3.83 (m, 8H), 4.04–4.16 (m, 12H), 6.86–6.99 (m, 4H), 7.02 (s, 2H), 7.13 (s, 1H), 7.47 (br s, 5H), 9.09 (br s, 2H); ¹³C NMR (75.5 MHz, CD₃SOCD₃): δ = 49.9, 50.0, 68.7, 69.0, 69.1, 70.4, 113.5, 114.0, 115.4, 121.1, 123.0, 124.2, 128.7, 129.0, 129.9, 132.0, 148.2, 148.4, 148.9; MS (LSD): *m/z* (%): 568 (51) [*M* – PF₆]⁺ and [2*M* – 2PF₆]²⁺, 590 (21) [*M* – H – PF₆ + Na]⁺, 700 (19) [*M* – H – PF₆ + Cs]⁺, 1135 (100) [2*M* – H – 2PF₆]⁺, 1281 (16) [2*M* – PF₆]⁺; C₃₂H₄₂NO₈PF₆ (713.6): calcd C 53.86, H 5.93, N 1.96; found C 53.60, H 5.84, N 2.05.

(2-Benzylammoniummethyl)dibenzo-24-crown-8 Trifluoroacetate (1-H·O₂CCF₃). A CH₂Cl₂ solution of the amine **1** was treated with an excess of CF₃CO₂H. Removal of the solvents in vacuo afforded **1-H·O₂CCF₃** as a pale yellow solid. Single crystals suitable for X-ray crystallographic analysis were obtained when a solution of the salt in EtOAc/C₆H₁₄/MeCN (10:10:1) was allowed to stand at 20 °C for approximately 1 d. Crystal data for C₃₂H₄₂NO₈·CF₃CO₂·CF₃CO₂H: *M_r* = 795.7, monoclinic, space group *C2/c*, *a* = 22.936 (4), *b* = 23.249 (3), *c* = 15.393 (3) Å, β = 112.14 (1)°, *V* = 7603 (2) Å³,

Z = 8, ρ_{calcd} = 1.39 g cm⁻³, μ (MoKα) = 1.22 cm⁻¹, *F*(000) = 3328. Crystal dimensions 0.33 × 0.33 × 0.80 mm (needles), Siemens P4 diffractometer, graphite-monochromated MoKα radiation, ω-scans, *T* = 203 K. Of 6449 independent reflections measured (2θ ≤ 50°), 2715 had *I_o* > 2σ(*I_o*) and were considered to be observed. The structure was solved by direct methods and the non-hydrogen atoms refined anisotropically. The positions of the NH₂⁺ hydrogen atoms were located from a Δ*F* map and refined isotropically subject to an N–H distance constraint. The remaining hydrogen atoms were placed in calculated positions, assigned isotropic thermal parameters *U*(H) = 1.2 *U*_{eq}(C), and allowed to ride on their parent atoms. Refinement was by full-matrix least-squares, based on *F*² to give *R*₁ = 0.092, *wR*₂ = 0.222. Computations were carried out using the SHELXTL 5.03 package.⁴² CCDC 100961.⁴³

1,2-Bis(2-{2-[2-(2-*p*-tolylsulfonyloxy)ethoxy]ethoxy}ethoxy)benzene (24). Diol **23**³⁸ (55.0 g, 147 mmol), Et₃N (74.3 g, 734 mmol) and a catalytic amount of 4-dimethylaminopyridine were dissolved in CH₂Cl₂ (400 mL), and this solution was stirred and cooled (0–5 °C). A solution of *p*-toluenesulfonyl chloride (61.6 g, 323 mmol) in CH₂Cl₂ (100 mL) was then added dropwise over a period of 2 h, maintaining the reaction temperature below 5 °C. Subsequently, the reaction mixture was allowed to warm to ambient temperature and left to stir for a further 3 h under a continuous flow of N₂. The reaction mixture was acidified with 5 M HCl solution (250 mL), and the organic layer was washed with 2 M HCl solution (2 × 200 mL). The organic layer was dried (MgSO₄), and the solvents were removed in vacuo. The residue was purified by filtering through a pad of SiO₂ (gradient elution with EtOAc/C₆H₁₄, 10:90 to 60:40) to yield the desired compound **24** as a pale yellow oil (82.8 g, 83%); ¹H NMR (200 MHz, CDCl₃): δ = 2.39 (s, 6H), 3.53–3.81 (m, 16H), 4.08–4.14 (m, 8H), 6.88 (s, 4H), 7.29 (d, *J* = 8.2 Hz, 4H), 7.75 (d, *J* = 8.2 Hz, 4H); ¹³C NMR (50 MHz, CDCl₃): δ = 21.6, 68.7, 68.9, 69.4, 69.8, 70.7, 115.0, 121.7, 127.9, 129.9, 133.0, 144.8, 149.0; MS (FAB): *m/z* (%): 682 (26) [*M*]⁺; C₃₂H₄₂O₁₂S₂ (682.8): calcd C 56.29, H 6.20; found C 56.39, H 6.17.

Benzo(5-hydroxymethylmetaphenylene)[25]crown-8 (26). Cesium carbonate (47.7 g, 146 mmol) was placed in a 2 L round-bottomed flask fitted with condenser and pressure-equalized dropping funnel. The system was flushed with N₂, and anhydrous MeCN (700 mL) was added to the flask. The ditosylate **24** (20.0 g, 29.3 mmol) and 3,5-dihydroxybenzyl alcohol (**25**) (4.10 g, 29.3 mmol) were dissolved in dry MeCN (600 mL) and added to the dropping funnel, again through a flow of N₂. The suspension in the flask was heated under reflux while stirring, and the ditosylate/**25** solution was added dropwise over 24 h. This mixture was stirred at reflux, under an N₂ atmosphere, for a further 3 d. Upon cooling, the reaction mixture was filtered, the solvent removed in vacuo, and the residue partitioned between CH₂Cl₂ (300 mL) and 10% w/v K₂CO₃ solution (300 mL). The aqueous layer was further extracted with CH₂Cl₂ (3 × 300 mL), and the combined organic layers were washed with 10% w/v K₂CO₃ solution (300 mL). The organic phase was dried (MgSO₄), and the solvents were removed in vacuo. The residue was subjected to column chromatography (SiO₂: EtOAc/C₆H₁₄, 90:10) to yield a white solid (4.50 g, 32%); mp 68–71 °C; ¹H NMR (400 MHz, CDCl₃): δ = 3.66–3.71 (m, 8H), 3.77–3.82 (m, 8H), 4.08–4.12 (m, 8H), 4.53 (s, 2H), 6.48 (d, *J* = 2.3 Hz, 2H), 6.57 (d, *J* = 2.3 Hz, 1H), 6.84–6.89 (m, 4H); ¹³C NMR (75 MHz, CDCl₃): δ = 65.1, 68.1, 68.9, 69.8, 69.9, 71.0, 101.7, 106.2, 115.1, 121.7, 143.5, 149.0, 160.1; MS (FAB): *m/z* (%): 461 (75) [*M* – OH]⁺, 478 (100) [*M*]⁺, 501 (6) [*M* + Na]⁺; C₂₅H₃₄O₉ (478.5): calcd C 62.75, H 7.16; found C 62.73, H 7.04.

Benzo(5-formylmetaphenylene)[25]crown-8 (27). PCC (3.68 g, 17.1 mmol) was added to a stirred solution of **26** (3.27 g, 6.83 mmol) in dry CH₂Cl₂ (150 mL). Although initially

(42) SHELXTL PC version 5.03, Siemens Analytical X-ray Instruments, Inc., Madison, WI, 1994.

(43) Copies of the crystallographic data can be obtained free of charge on application to CCDC, 12 Union Road, Cambridge CB12 1EZ, UK (Fax: (+44) 1223–336033; E-mail: teched@ccdc.cam.ac.uk).

orange, the solution very quickly went black and was stirred for a further 75 min. After this time, the reaction mixture was filtered through a small layer of Celite, which was then washed with CH_2Cl_2 (500 mL). The green CH_2Cl_2 filtrate was stirred with 200 mL aliquots of 2 N NaOH solution until colorless and subsequently dried (MgSO_4), and the solvent was removed in vacuo to yield a colorless oil. This oil was dissolved in EtOAc and precipitated with C_6H_6 to afford the desired compound (**27**) as a powdery white solid (2.55 g, 78%); mp 68–69 °C; ^1H NMR (500 MHz, CDCl_3): δ = 3.69–3.74 (m, 8H), 3.82–3.86 (m, 8H), 4.12–4.21 (m, 8H), 6.86–6.91 (m, 4H), 6.96–7.00 (m, 3H), 9.84 (s, 1H); ^{13}C NMR (125 MHz, CDCl_3): δ = 68.6, 69.1, 70.0, 70.1, 71.2, 71.3, 108.9, 109.3, 115.4, 121.9, 138.4, 149.2, 160.7, 192.1; MS (FAB): m/z (%): 476.5 (100) [M] $^+$; $\text{C}_{25}\text{H}_{32}\text{O}_9$ (476.5); calcd C 63.01, H 6.77; found C 62.89, H 6.80.

(5-[Benzylammoniummethyl]metaphenylene)[25]-crown-8 Hexafluorophosphate (22-H·PF₆). A solution of the formyl-substituted crown ether **27** (685 mg, 1.44 mmol) and benzylamine (**10**) (154 mg, 1.44 mmol) in PhMe (50 mL) was heated under reflux for 24 h using a Dean–Stark apparatus. The resulting solution was evaporated to dryness, the residue was dissolved in dry MeOH (100 mL), and NaBH_4 (272 mg, 7.19 mmol) was added portionwise over a period of 5 min. After being stirred under ambient conditions for 24 h, the reaction mixture was evaporated to dryness, and the residue was partitioned between NaOH solution (2 N, 200 mL) and CH_2Cl_2 (200 mL). The aqueous layer was further extracted with CH_2Cl_2 (2 × 250 mL), the combined organic extracts were dried (MgSO_4), and the resulting solution was evaporated to dryness to yield an off-white solid. The solid was subsequently dissolved in MeOH (100 mL), and 12 M HCl solution (10 mL)

was added carefully. After stirring for ca. 10 min, the solvents were removed in vacuo, and the residue dissolved in hot H_2O . Addition of an excess of saturated aqueous NH_4PF_6 to this solution resulted in the precipitation of a white solid. Upon collection, the solid was dissolved in CH_2Cl_2 , and precipitated with Et_2O to afford the desired compound as a powdery white solid (152 mg, 15%); mp 177–179 °C (decomp); ^1H NMR (400 MHz, CD_3SOCD_3): δ = 3.56–3.62 (m, 8H), 3.69–3.85 (m, 8H), 4.03–4.09 (m, 6H), 4.13–4.17 (m, 6H), 6.65 (d, J = 2.0 Hz, 2H), 6.71 (t, J = 2.0 Hz, 1H), 6.84–6.89 (m, 2H), 6.92–6.98 (m, 2H), 7.36 (s, 1H), 7.39–7.50 (m, 5H), 9.12 (br s, 2H); ^{13}C NMR (125 MHz, CD_3SOCD_3): δ = 50.1, 67.7, 68.1, 69.1, 70.1, 70.2, 102.3, 108.9, 114.3, 121.2, 128.7, 129.1, 130.0, 131.8, 133.7, 148.3, 159.8; MS (FAB): m/z (%): 568.4 (100) [$M - \text{PF}_6$] $^+$, 1135.6 (3) [$2M - \text{H} - 2\text{PF}_6$] $^+$; $\text{C}_{32}\text{H}_{42}\text{NO}_8\text{PF}_6$ (713.6): calcd C 53.86, H 5.93, N 1.96; found C 53.47, H 5.85, N 1.86.

Acknowledgment. This research was supported by the National Science Foundation. Anthony Pease is thanked for producing the ray-traced pictures contained within this paper.

Supporting Information Available: Additional synthetic schemes, supporting diagrammatic and spectroscopic figures, supporting experimental data, and a mathematical model for the aggregation of self-complementary daisy chain molecules. This material is available free of charge via the Internet at <http://pubs.acs.org>.

JO010405H